Modeling and Performance Evaluation of 3GPP LTE Channel Encoder/Decoder

Dissertation submitted in the partial fulfilment of
requirements for the award of degree of

Master of Technology
in
VLSI Design & CAD

Submitted By
Dolesh Bhardwaj
Roll No: 601161030

Under the guidance of
Mr. H. K. S. Randhawa
Assistant Professor, ECED
Thapar University, Patiala

Department of Electronics and Communication Engineering
THAPAR UNIVERSITY
PATIALA – 147004, PUNJAB, INDIA

July, 2013

DECLARATION

I, **Dolesh Bhardwaj**, hereby certify that the work which is being presented in this thesis entitled **"Modeling and Performance Evaluation of 3GPP LTE Channel Coder/Decoder"** by me in partial fulfillment of the requirements for the award of degree of Master of Technology in VLSI Design & CAD from Thapar University (Deemed University), Patiala, is an authentic record of my own work carried out under the supervision of **Mr. H. K. S. Randhawa**, Assistant Professor, ECED, Thapar University, Patiala.

The matter presented in this thesis has not been submitted in any other University / Institute for the award of any other degree.

Date: 15/07/13.

Dolesh Bhardwaj
Roll No. 601161030

It is certified that the above statement made by the student is correct to the best of my knowledge and belief.

Date:

Mr. H. K. S. Randhawa
Assistant Professor
ECED

Countersigned by:

Dr. Rajesh Khanna
Professor and Head ECED
Thapar University, Patiala
Date:

Dr. S. K. Mohapatra
Dean of Academic Affairs
Thapar University, Patiala
Date:

ACKNOWLEDGEMENT

I would like to express my sincere gratitude to my supervisor **Mr. H. K. S. Randhawa, Assistant Professor**, Electronics and Communication Engineering Department, for his invaluable guidance, inspiration and discussions through all stages of this research work to complete the dissertation in time. I am greatly indebted to him for encouragement and support without which, it would not have been possible for me to complete this undertaking successfully. I am truly very fortunate to have the opportunity to work with him. His insightful comments and suggestions have continually helped me to improve my understanding.

My sincere thanks are due to **Dr. Rajesh Khanna**, **Head of the Department** of Electronics and Communication Engineering for providing the constant encouragement and providing the facilities in the department for the completion of dissertation work. I also express my gratitude towards **Dr. Kulbir Singh**, **PG Coordinator**, Department of Electronics and Communication Engineering for his valuable guidance and encouragement.

My gratitude goes to **Dr. Sanjay Sharma**, **Professor**, Department of Electronics and Communication Engineering who supported and guided me throughout my dissertation with many valuable suggestions and helpful discussions while allowing me the room to work in my own way. This dissertation would not have been possible without their guidance, encouragement and trenchant critiques.

I would like to thank entire faculty and staff of Electronics and Communication Engineering Department and then friends who devoted their valuable time and helped me in all possible ways towards successful completion of this work. I thank all those who have contributed directly or indirectly to this work.

I take pride of myself being son of ideal parents for their over lasting desire, sacrifice, affection blessings and help without which it would not have been possible for me to complete my studies.

Last but not least, I would like to thank God for all good deeds.

Dolesh Bhardwaj

ABSTRACT

Long Term Evolution (LTE) of the Universal Mobile Telecommunication System (UMTS) also known as the Evolved Packet System (EPS) is a transilient move in the field of mobile communications. Such a revolution is necessitated by the unceasing increase in demand for high speed connections on networks, low latency and delay, low error rates and resilience because modern users and network applications have become increasingly dependent on these requirements for efficient functionality and performance. Third Generation Partnership Project Long Term Evolution (3GPP LTE) promises high peak data rates for both uplink and downlink transmission, spectral efficiency, low delay and latency, and low bit error rates. These functional and performance targets of 3GPP LTE are laudable and can be met with a great measure of certainty, but then a vital question emerges: What are the prime drivers or enablers for these technology standard requirements to be met? LTE leverages on a number of technologies namely Multi Input Multiple Output (MIMO) antennas, Orthogonal Frequency Division Multiplexing (OFDM) and Orthogonal Frequency Division Multiple Access (OFDMA) at the downlink, Single Carrier Frequency Division Multiple Access (SCFDMA) at the uplink, support for Quadrature Phase Shift Keying (QPSK), 16 Quadrature Amplitude Modulation (16QAM), and 64QAM.

This dissertation work evaluates the performance of 3GPP LTE downlink channel coding and decoding. The performance metrics considered are throughput versus SNR and BLER versus SNR and these are used to evaluate the performance of LTE channel coding and decoding. The granular analysis and evaluation of the performance 3GPP LTE is imperative and this dissertation implements this on the downlink side. A thorough analysis and performance evaluation of the LTE downlink with channel coding/decoding is thus the focal point and the results demonstrate that the design goals and requirements of 3GPP LTE can be met with a great deal of reliability and certainty.

***Keywords*:** 3GPP LTE, 16QAM, 64QAM, MIMO, OFDM, OFDMA, SC-FDMA, UMTS, TDD, FDD.

TABLE OF CONTENTS

LIST OF FIGURES

LIST OF TABLES

LIST OF ACRONYMS

3GPP	Third Generation Partnership Project
ARQ	Automatic Repeat Request/Query
BER	Bit Error Rate
BLER	Block Error Rate
BS	Base Station
CP	Cyclic Prefix
DFT	Discrete Fourier Transform
DL	Downlink
EPS	Evolved Packet System
E-UTRAN	Evolved UTRAN
FFT	Fast Fourier Transform
FDD	Frequency Division Duplex
FDM	Frequency Division Multiplexing
FDMA	Frequency Division Multiple Access
HARQ	Hybrid ARQ
HSDPA	High Speed Downlink Packet Access
HSPA	High Speed Packet Access
IDFT	Inverse Discrete Fourier Transform
IFFT	Inverse Fast Fourier Transform
ISI	Inter Symbol Interference
LTE	Long Term Evolution
MIMO	Multiple Input Multiple Output
PRB	Physical Resource Block
OFDM	Orthogonal Frequency Division Multiplexing
OFDMA	Orthogonal Frequency Division Multiple Access
QAM	Quadrature Amplitude Modulation

QoS	Quality of Service
SAE	System Architecture Evolution
SC-FDMA	Single Carrier Frequency Division Multiple Access
SFBC	Space Frequency Block Coding
SISO	Single Input Single Output
SM	Spatial Multiplexing
TD	Transmit Diversity
TDD	Time Division Duplex
TTI	Transmission Time Interval
UE	User Equipment
UL	Uplink
UTRAN	UMTS Terrestrial Radio Access Network

CHAPTER

1 INTRODUCTION

1.1 Background

LTE (Long Term Evolution) is a new high performance air interface for cellular mobile communication systems developed by the 3rd Generation Partnership Project (3GPP), collaboration between groups of telecommunications associations. LTE represents a major advance in cellular technology. It is the next step in a continuous move to wider bandwidths and higher data rates. LTE is expected to be the next major standard in mobile broadband technology that promises to enhance the delivery of mobile broadband services through a combination of very high transmission speed, more flexible and efficient use of spectrum, and reduced packet latency.

The demand for high speed and widespread network access in mobile communications increases everyday as the number of users increases and applications are constantly developed with greater demand for network resources. As a result of this trend, mobile communications has experienced significant developments within the last two decades which is the result of tremendous research that have been carried out.

The 3rd Generation Partnership Project Long Term Evolution (3GPP LTE) is the system that marks the evolutionary move from third generation of mobile communication i.e. Universal Mobile Telecommunication System (UMTS) to fourth generation mobile technology. The first work on LTE began in release 7 of the 3GPP UMTS specifications involving the completion of its feasibility studies. This release also included further improvements on High Speed Packet Access (HSPA). Specification of LTE and System Architecture Evolution (SAE) constitutes the main work done in release 8 of the 3GPP UMTS specifications. As at the time of writing, work is currently in progress for the enhancement of LTE which is featured in release 10 of the 3GPP UMTS specifications and named LTE-Advanced (LTE-A). A comprehensive summary of the evolutionary trend of the 3GPP UMTS is given in Table 1.1 [1, 2]. Under the 3G/UTRAN (Universal

Terrestrial Radio Access Network) evolution study item, LTE was initially referred to as the Evolved UTRAN access network in 3GPP reports, documents, and specifications. On the Core Network side (CN), the evolution towards the Evolved Packet Core (EPC) is known as the SAE. The Evolved UMTS is thus the combination of the E-UTRAN access network and the EPC Core Network, known as 3GPP UMTS in standard documents [3].

Table 1.1: Evolution of the UMTS Specifications [2].

Release	Functional freeze	Main UMTS feature of release
Rel-99	March 2000	Basic 3.84 Mcps W-CDMA (FDD & TDD)
Rel-04	March 2001	1.28 Mcps TDD (aka TD-SCDMA)
Rel-05	June 2002	HSDPA
Rel-06	March 2005	HSUPA (E-DCH)
Rel-07	December 2007	HSPA+ (64QAM downlink, MIMO, 16QAM uplink) LTE and SAE feasibility study
Rel-08	December 2008	LTE work item – OFDMA/SC-FDMA air interface SAE work item – new IP core network Further HSPA improvements
Rel-09	December 2009	SAES Enhancements, WiMAX and LTE/UMTS Interoperability.
Rel-10	March 2011	LTE Advanced fulfilling IMT Advanced 4G requirements.
Rel-11	September 2012	Advanced IP Interconnection of Services.
Rel-12	In progress	Content still open (as of October 2012)

1.1.1 A Brief History of 3GPP Long Term Evolution (LTE)

The first of the wireless technologies to emerge were analog radios practically. These 1st generation networks developed in 1980s had two main wireless technologies; Advanced Mobile Phone System (AMPS) in United States and Nordic Mobile Telephone (NMT) in Europe. Global System for Mobile Communications (GSM) evolved of these 1st generation technologies with a major step ahead towards the digital radio. The features such as Short Message Service (SMS), Multimedia Message Service (MMS), Voice Message Service (VMS) and Value Added Services (VAS) made it one of the most used technologies in the world. This firmly established it as a leader in the 2nd generation

network. Other competing technologies were IS-95 Code Division Multiple Access (CDMA), Time Division Multiple Access (TDMA) and Personal Digital Cellular (PDC).

The network was expanded to include the data service with the addition of General Packet Radio Service (GPRS). Based on Release 97 (R'97) specifications, GPRS delivered 20 kbps in downlink and 14 kbps in uplink. Enhancements made on Releases R'98 and R'99 increased the theoretical downlink speed to 171 kbps. Addition of GPRS to GSM places it in between the 2nd generation and the 3rd generation. It is often referred to as 2.5G. Enhanced Data rates for GSM Evolution (EDGE) extended the data services of GSM further up to 384 kbps at max terming the network to 2.75G [4].

UMTS can be presented as the 3rd generation network evolved of the 2nd generation GSM networks. Its specification was developed by 3GPP and commercially launched for the first time in Japan in 2001. UMTS is based on Wideband CDMA (WCDMA) technology where the user data is multiplied by a high speed chip of 3.84 Mcps to obtain a code division multiplexed output. The radio interface of UMTS is architecturally similar to GSM network although there are distinct differences that make UMTS radio interface unique.

UMTS was succeeded by HSPA which introduced a higher downlink throughput with High Speed Downlink Packet Access (HSDPA) providing theoretical peak downlink data rate of 14.4 Mbps compared to theoretical limit of 2 Mbps for UMTS. High Speed Uplink Packet Access (HSUPA) in the uplink path provides the theoretical peak uplink data rate of 5.7 Mbps. HSPA+ was also introduced with enhanced data rates over preceding HSPA with theoretical data rate extending up to 84 Mbps in downlink and 22 Mbps in uplink [5].

While the implementation of UMTS was ongoing, 3GPP also initiated research on the Long Term Evolution of UMTS Network predicting the increase in the bandwidth demands from the consumer as well as high-end web applications on wireless devices. The motive was mainly to shift current networking trend to an IP switched network. First workshop for LTE was conducted by 3GPP on November 2004 in Canada. Study and research was made on LTE to make it a part of the 3GPP Release 8 Specification. By March 2009, the Protocol freezing was made and the specifications were baselined by 3GPP.

1.2 3GPP Long Term Evolution (LTE) in Modern World

Long Term Evolution (LTE) is a next generation wireless communication system which uses Orthogonal Frequency Division Multiple Access (OFDMA) and Single Carrier - Frequency Division Multiple Access (SC-FDMA) in downlink and uplink respectively. In the present era to achieve the design goals of LTE it must satisfy the following requirements:

- **Data rates:** LTE should support a data rate up to 100 Mb/s within a 20 MHz downlink spectrum allocation and 50 Mb/s within a 20 MHz uplink or, equivalently, spectral efficiency values of 5 bps/Hz and 2.5 bps/Hz, respectively.
- **Throughput:** The downlink average throughput per MHz is about 3 to 4 times higher than in the release 6. The uplink average user throughput per MHz is about 2 to 3 times higher than in the release 6.
- **Bandwidth:** LTE allows bandwidth ranging from 1.4 MHz up to 20 MHz, where the latter is used to achieve the highest LTE data rate. Furthermore, LTE operates in both paired and unpaired spectrum by supporting both Frequency Division Duplex (FDD) and Time Division Duplex (TDD).
- **Mobility:** The mobility is optimized for low terminals speeds ranging from 0 to 15 km/h. The connection should be maintained for very high UEs speed up to 350 km/h or even up to 500 km/h.
- **Coverage:** The above targets should be met for 5 km cells and some slight degradation in throughput and spectrum efficiency for 30 km cells. 100 km cells and up can’t meet the targets requirements.

1.3 LTE Performance Targets

The design goals for LTE is to provide downlink peak rates of 100 Mbps and uplink of 50 Mbps, to exhibit spectral efficiency and flexibility by supporting scalable bandwidth which enhances the provision of more data and voice services over a given bandwidth. A fundamental goal of 3GPP LTE is to provide a high data rate with low latency in both theory and practice. Summary of key performance requirement of LTE for uplink and downlink is shown in Table 1.2 below.

Table 1.2: Performance targets for Long Term Evolution.

		Requirements	**Comments**
Downlink	Peak data transmission rate	> 100 Mbps	LTE Bandwidth = 20 MHz Duplexing Mode = FDD Spatial Multiplexing = 2x2
	Peak Spectral Efficiency	> 5 b/s/Hz	
	Spectral Efficiency of cell Edge	> 0.04 – 0.06 bps/Hz/user	Assumed 10 Users/Cell
	Average Cell Spectral Efficiency	> 1.6 – 2.1 bps/Hz/cell	Spatial Multiplexing = 2x2 Receiver = IRC (Interference Rejection Combining)
	Broadcost Specral Efficiency	1 bps/Hz	Carrier dedicated for Broadcast mode
		Requirements	**Comments**
Uplink	Peak Data Transmission Rate	> 50 Mbps	LTE Bandwidth = 20 MHz Duplexing Mode = FDD Transmission = Single Antenna
	Peak Spectral Efficiency	> 2.5 bps/Hz	
	Spectral Efficiency of Cell Edge	> 0.02 – 0.03 Bps/Hz/user	Single Antenna transmission Receiver =IRC
	Average Spectral Efficiency	> 0.66 – 1.0 bps/Hz/cell	Assumed 10 Users/Cell
System	Operating Bandwidth	1.4 MHz to 20 MHz	Initially starts at 1.25 MHz
	User Plane Latency	< 10 ms	High throughput
	Connection set up Latency	< 100 ms	From Idle mode to Active

1.4 LTE Physical Layer

The physical layer of LTE conveys data and control information between E-UTRAN NodeB (eNodeB) and user equipment (UE) in an efficient way. It employs advanced technologies such as OFDM and MIMO for data transmission. In addition, LTE uses OFDMA and SC-FDMA for downlink and uplink data transmissions. The use of SC-FDMA in the uplink reduces PAPR. A detail description of LTE physical layer is provided below.

1.4.1 LTE Generic Frame Structure

The generic frame of LTE has a length of 10ms and is subdivided into ten sub-frames of 1ms length. Each sub-frame is further divided into two slots of 0.5ms having six or seven OFDM symbols depending upon the length of CP. Each slot uses 7 OFDM symbols in case of normal CP whereas 6 OFDM symbols in case of extended CP. Sub-frames can be assigned for either uplink or downlink. The generic frame structure of LTE downlink and uplink is shown in Fig. 1.1.

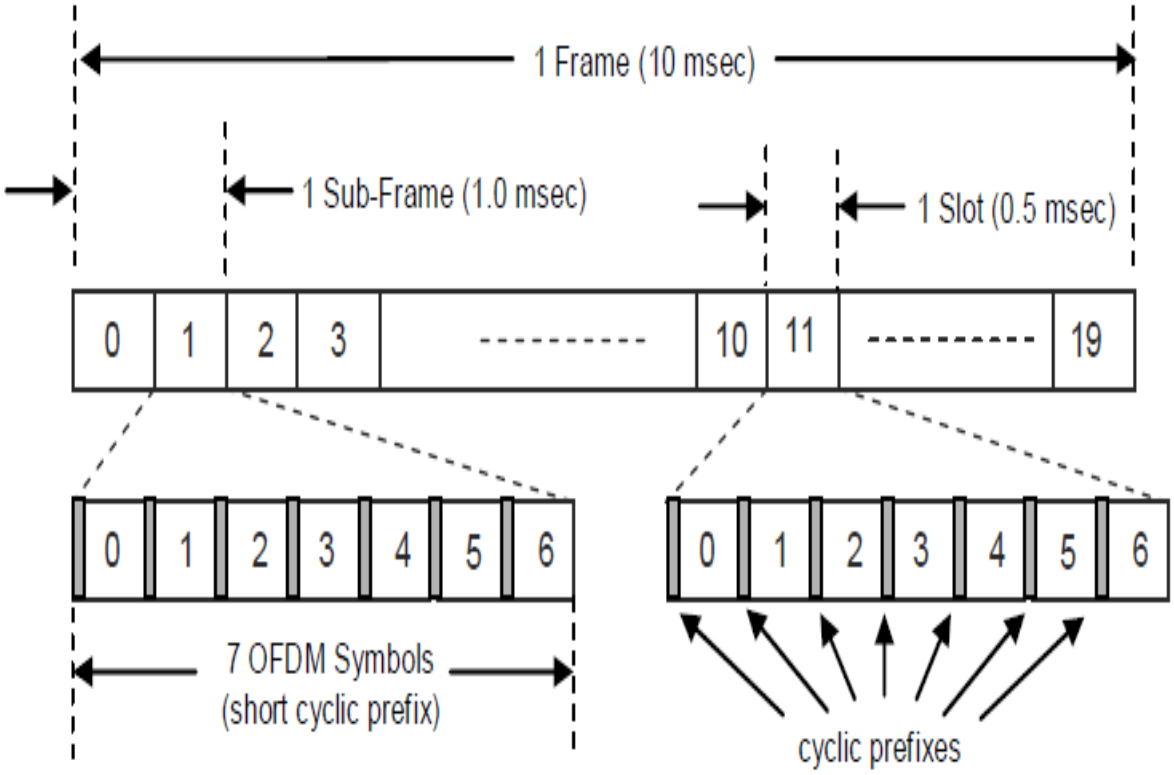

Figure 1.1: Generic Frame Structure for Downlink and Uplink of LTE.

1.4.2 LTE Physical Layer for downlink Transmission

1.4.2.1 Modulation Parameters

The transmission scheme used in downlink is OFDM using a cyclic prefix. The basic subcarrier spacing is 15 kHz with OFDM symbol duration of 66.67us. The downlink uses a subcarrier spacing of 7.5 kHz with OFDM symbol duration of 133us in case of Mobile Broadcast Single Frequency Network (MBSFN). MBSFN refers to a mobile network using a single band on which broadcasted and dedicated signals are sharing single frequency [8]**.** Two types of cyclic prefixes are used, depending on the delay dispersion characteristics of the radio cell (channel delay spread). The normal CP is used in urban or high frequency areas whereas extended CP is used in rural and low frequency areas.

The modulation parameters for various transmission bandwidth configurations for LTE are shown in Table 1.3.

Table 1.3: Modulation Parameters for Downlink [8].

Transmission BW	1.4 MHz	3 MHZ	5 MHz	10 MHz	15 MHz	20 MHz
Sub-frame duration	0.5 ms					
Sub-carrier spacing	15 KHz					
Sampling frequency	1.92 MHz	3.84 MHz	7.68 MHz	15.36 MHz	23.04 MHz	30.72 MHz
FFT size	128	256	512	1024	1536	2048
Number of occupied subcarriers	72	180	300	600	900	1200
Number of OFDM symbols per slot (S/L)	7/6					
CP length (μs/samples) (S/L)	(4.69/9). 6	(4.69/18) . 6	(4.69/36). 6	(4.69/72). 6	(4.69/108) . 6	(4.69/144) . 6
	16.67/32	16.67/64	16.67/128	16.67/256	16.67/384	16.67/512

1.4.2.2 Downlink Physical Resource

The downlink physical resource consists of Physical Resource Blocks (PRBs) where a PRB consists of 12 consecutive subcarriers for one slot (1 slot = 0.5msec). The

bandwidth of PRB is 180 kHz. A resource element corresponds to one subcarrier for the duration of one OFDM symbol. Thus depending on the cyclic prefix length, a PRB comprises 84 OFDM symbols in case of normal CP and 72 OFDM symbol in case of extended CP. The number of resource blocks depends upon the transmission bandwidth of LTE i.e. 1.4 MHz to 20 MHz. Table 1.4 shows the number of PRBs for various transmission bandwidths.

Table 1.4: Number of Physical Resource Blocks (PRB) for Various Transmission Bandwidths [6].

Transmission Bandwidth (MHZ)	1.4	3	5	10	15	20
Subcarrier BW (kHz)	15					
PRB BW (kHz)	180					
Number of available PRB	6	15	25	50	75	100

The Downlink physical resource in time frequency grid is shown in Fig. 1.2 [7]. Fig. 1.2 shows that, a PRB is comprised of 12 consecutive subcarriers with a subcarrier spacing of 15 kHz and 7 OFDM symbols for the duration of 0.5ms in case of normal cyclic prefix. Thus a PRB of 84 resource elements (12 x7 = 84) corresponds to one slot in the time domain whereas a PRB of 180 kHz (15 kHz x 12 = 180 kHz) corresponds to the frequency domain.

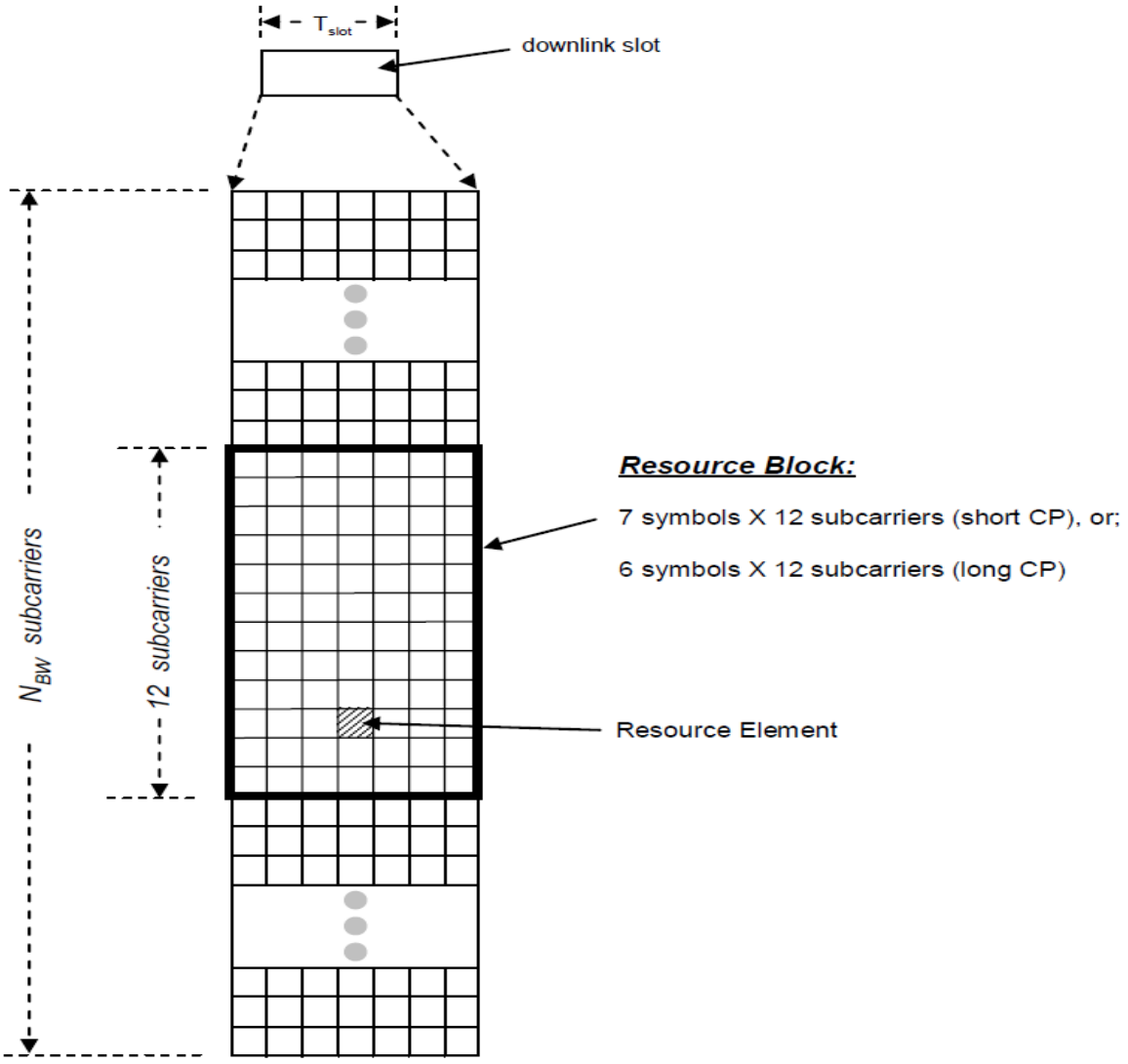

Figure 1.2: LTE Downlink Physical Resource [7].

1.4.2.3 Orthogonal Frequency Division Multiplexing (OFDM)

Orthogonal Frequency Division Multiplexing (OFDM) has gathered much attention in recent years and has been adopted as the downlink transmission scheme for the 3GPP LTE. OFDM is a multicarrier transmission scheme because it splits up the transmitted high bit-stream signal into different sub-streams and sends these over many different sub-channels. In other words OFDM simply divides the available bandwidth into multiple narrower sub-carries and transmits the data on these carries in parallel streams. Each subcarrier is modulated using different levels of modulation, e.g. QPSK, QAM, 64QAM and an OFDM symbol is obtained by adding the modulated subcarrier signals.

Advantages and Drawbacks of OFDM

This section summarizes the strengths and weaknesses of multi-carrier modulation based on OFDM.

Advantages:

- High spectral efficiency due to nearly rectangular frequency spectrum for high numbers of sub-carriers.
- Simple digital realization by using the FFT operation.
- Low complex receivers due to the avoidance of ISI and ICI with a sufficiently long guard interval.
- Flexible spectrum adaptation can be realized.
- Different modulation schemes can be used on individual sub-carriers which are adapted to the transmission conditions on each sub-carrier.

Disadvantages:

- Multi-carrier signals with high peak-to-average power ratio (PAPR) require high linear amplifiers. Otherwise, performance degradations occur and the out-of-band power will be enhanced.
- Loss in spectral efficiency due to the guard interval.
- More sensitive to Doppler spreads than single-carrier modulated systems.
- Phase noise caused by the imperfections of the transmitter and receiver oscillators influences the system performance.
- Accurate frequency and time synchronization is required.

1.5 Single Carrier-FDMA (SC-FDMA)

Long Term Evolution (LTE) uses OFDM as a strong modulation technique in the downlink transmission. The main drawback of OFDM is high peak to average power ratio which is overcome by SC-FDMA. Single Carrier-FDMA (SC-FDMA) is an extension of OFDMA and is used in the uplink of LTE. Unlike OFDMA, SC-FDMA reduces the PAPR by adding additional blocks of DFT and IDFT at transmitter and receiver.

1.6 Motivation

The motivation to work on this project comes from the fact that LTE is the future of mobile broadband. It is expected that in the future 80% of all mobile broadband users will be served by LTE [8]. The increasing demand for multimedia applications (e.g. HDTV,

video conferencing, video telephony and video-on-demand), motivates the need for designing a robust and reliable channel coding scheme over wireless channels.

On the other hand, wireless channels are characterized by their limited bandwidth and time varying nature which poses other challenges on multimedia communications. Moreover, data transmission over wireless channels is susceptible to random bit errors due to a number of impairments, such as path loss, shadowing and multipath fading. Therefore, when a compressed bit stream is transmitted over such error prone channels, the impact of bit errors might range from negligible, moderate, to extremely severe. Sometimes a single error could render a whole bit stream useless and might lead to the drop of the entire frame which robust typically degrades the quality of reconstructed information.

In multimedia communications, distortion in the reconstructed information can be classified into two types. The first type is the quantization distortion introduced by the lossy source encoding schemes and the second type is distortion due to channel errors. There are different ways to protect data against channel errors. Error control schemes at the highest level can be divided into two classes, namely, Automatic Repeat Request (ARQ) and Forward Error Correction (FEC). In ARQ schemes, a data block is encoded for error detection and when an error is detected at the receiver then retransmission is requested. Thus, these schemes are not suitable for time sensitive applications. The other viable option is employing FEC where a data block is encoded for error correction at the receiver without retransmission. However, FEC schemes add overhead data to provide the necessary correction capability. Clearly, this results a reduction in the effective data rate.

1.6.1 Importance of Channel Coding/Decoding in 3GPP LTE

One of the most important issues in digital communication systems is error detection and correction. Error correction can be considered in two main categories: ARQ (Automatic Repeat Request) and FEC (Forward Error Correction). With ARQ the receiver requests retransmission of the data packets, if errors are detected and this will be done, until the received packets are error-free or a maximum number of retransmissions are reached.

For FEC redundancy bits are added to data bits, making error correction possible. FEC has two main types: block codes and convolutional codes. In block codes, the input data blocks, which can be considered as vectors are multiplied by a generator matrix, generating a code word vector. In contrast to block codes, convolutional codes have a

similar structure like FIR (Finite Impulse Response) filters and operate bitwise. Convolutional codes have memory, which means the coded output bit depends not only on the current bit but also on the m previous bits, where m is the number of registers in the convolutional encoder. In LTE both block codes and convolutional codes are used. CRC (Cyclic Redundancy Check) which is a cyclic linear block code is used for ARQ as an error correction technique. Control channels and data channels in LTE use convolutional and Turbo codes, respectively, where the later is an enhanced development of convolutional codes achieving near-Shannon performance. Hence to detect and correct the error channel coding and decoding become an integral part of 3GPP Long Term Evolution (LTE).

1.7 LTE Downlink Channel Coding/Decoding

Channel coding is a method to reduce information rate and increase the reliability of channel by adding redundancy to the information symbol vector resulting in a longer coded vector of symbols that are distinguishable at the output of the channel this goal is achieved.

The current LTE systems use turbo coding scheme, but due to the high peak data rates supported by LTE [9], it becomes imperative to know if this same turbo coding scheme can scale to high data rates while maintaining reasonable decoding complexity. It is currently debated that turbo coding has a particular drawback that it is not amenable to parallel implementations which limit the achievable decoding speeds. The underlying reason behind this issue is the contention for memory resources among parallel processors which occurs as a result of the turbo code internal interleaver. On the other hand, it is argued that turbo codes can also employ parallel implementations if turbo internal interleavers can be made contention-free.

The LTE air interface consists of physical channels and physical signals which are generated by the LTE physical layer. Physical channels carry data from higher layers including control, scheduling and user payload and physical signals are used for system synchronization, cell identification and radio channel estimation. The types of downlink physical channels are Physical Downlink Shared Channel (PDSCH), Physical Broadcast Channel (PBCH), Physical Multicast Channel (PMCH), Physical Control Format Indicator Channel (PCFICH), Physical Downlink Control Channel (PDCCH) and Physical Hybrid ARQ Indicator Channel (PHICH). The types of uplink physical channels

are PRACH (Physical random access channel), PUCCH (Physical uplink control channel) and PUSCH (Physical uplink shared channel). In LTE Convolutional coding is used for control channel and Turbo coding is used for shared channel.

In control channels like Physical Downlink Control CHannel (PDCCH) and Physical Broadcast CHannel (PBCH) a convolutional code is used. The reason is that the code blocks are much more smaller than in data channels and for small blocks the Turbo codes internal interleaver does not work efficiently. Because of the small number of bits carried in PDCCH and PBCH and in order to avoid overhead, the tail-biting approach instead of inserting tail bits is used as terminating method. The initial value of the shift register of the encoder shall be set to the values corresponding to the last 6 information bits in the input stream so that the initial and final states of the shift register are the same. The decoder can be either a circular Viterbi algorithm or a MAP algorithm. The rate-matching for the convolutional code in LTE uses a similar circular buffer method as for the Turbo code.

1.8 Objectives

The following are the main objectives of this dissertation work:

1. To develop a channel coding/decoding model for 3GPP Long Term Evolution (LTE).
2. To simulate the developed channel coding/decoding model for 3GPP LTE.
3. To evaluate the performance of channel coding/decoding model in terms of throughput versus Signal to Noise Ratio (SNR) and Block Error Rate (BLER) vs SNR.

1.9 Outline of the Dissertation

Following the introduction **(Chapter 1)** the dissertation is organized as follows:

Chapter 2 is dedicated to literature review. The research papers which are relevant to this dissertation are discussed here and this chapter surveys some important studies in the field of our research and outlines the main ideas contained in them.

Chapter 3 describes the proposed performance evaluation channel coding and decoding model with Hybrid Repeat Request (HARQ) for 3GPP LTE using SystemVue softwere.

Chapter 4 shows the simulation results and performance analysis of proposed 3GPP LTE channel coding/decoding model using plots throughput versus Signal to Noise Ratio

(SNR) and Block Error Rate (BLER) versus Signal to Noise Ratio (SNR) which are simulated in SystemVue softwere for different modulation schemes such as QPSK, 16QAM and 64QAM.

Chapter 5 concludes the dissertation and proposes the future work to be done in order to continue the investigation performed in this dissertation.

CHAPTER

2

LITERATURE REVIEW

Different characteristics and features of LTE have been presented in the literature. Most of the research on LTE started in 2007 since the first release of this standard by 3GPP. This chapter provides a brief review on publications in different journals and conferences. Since the main objective of this study is modelling and performance evaluation of LTE downlink channel coding and decoding, the literature review is related but not limited to materials regarding performance, features and techniques of the channel coding and decoding.

Channel coding is a method to reduce information rate and increase the reliability of channel by adding redundancy to the information symbol vector resulting in a longer coded vector of symbols that are distinguishable at the output of the channel this goal is achieved.

The current LTE systems use turbo coding scheme, but due to the high peak data rates supported by LTE [9], it becomes imperative to know if this same turbo coding scheme can scale to high data rates while maintaining reasonable decoding complexity. It is currently debated that turbo coding has a particular drawback that it is not amenable to parallel implementations which limit the achievable decoding speeds. The underlying reason behind this issue is the contention for memory resources among parallel processors which occurs as a result of the turbo code internal interleaver. On the other hand, it is argued that turbo codes can also employ parallel implementations if turbo internal interleavers can be made contention-free.

A coding scheme that possesses inherent parallelism and therefore offers high decoding speeds is the Low Density Parity Check (LPDC) code which is currently increasing in availability. LPDC potential offers opportunities to achieve very high throughput which is made possible as a result of its inherent parallelism of the decoding algorithm while maintaining good error-correcting performance and low decoding complexity.

2.1 Channel Coding in LTE

The preferred channel coding for LTE is turbo coding. This selection in favour of turbo coding is based on few reasons:

- UMTS release 6 HSPA also uses turbo code.
- For backward compatibility reasons, dual-mode LTE terminals will need to implement turbo code therefore some decoding hardware can be reused.
- To avoid increased implementation complexity as the terminals have to support two different coding schemes.

There are some major channel coding schemes used in the LTE system [9]:

- Turbo coding: Chiefly used for large data packets which common occurrence in downlink and uplink data transmission, paging and broadcast multicast (MBMS) transmissions, in other words, for Uplink shared channel (UL-SCH), downlink shared channel (DL-SCH), Paging Channel (PCH) and Multicast Channel MCH [2, 10].
- Rate 1/3 convolutional coding mainly used for downlink control and uplink control as well as broadcast control channel [2].

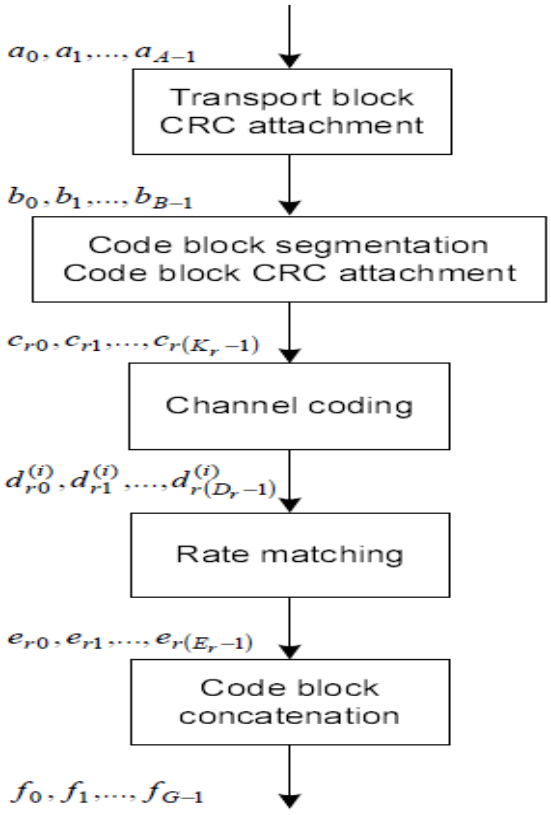

Figure 2.1: Transport block processing [2].

Fig. 2.1 shows the processing structure for each transport block for the DL-SCH, PCH and MCH transport channels. Data arrives to the coding unit in the form of a maximum of two transport blocks every transmission time interval (TTI) per DL cell. The following coding steps can be identified for each transport block of a DL cell:

- Add CRC to the transport block
- Code block segmentation and code block CRC attachment
- Channel coding
- Rate matching
- Code block concatenation

2.2 LTE Specifications and Features

A comprehensive description of the link layer protocols and the interaction between protocol layers is discussed by ***A. Larmo, et al.*** [11]. Compared with other UTRAN protocols, LTE provides less delay and overhead. Moreover, the interaction between protocol layers is more efficient. For example, the Medium Access Control (MAC) and Radio Link Control (RLC) layers interact with each other with two layer Automatic Repeat request (ARQ) functionalities, and scheduling in MAC and segmentation in RLC are interworking properly. As a result of appropriate layer interactions, the LTE protocol header has low overhead. Furthermore, UE advanced sleep mode and handover techniques are described and outlined.

D. Astely, et al. [12], gives an overview of LTE characteristics and study different features such as physical layer specifications, multi antenna transmission, and intra-cell interference coordination. Moreover, LTE spectral efficiency for uplink and downlink is evaluated under specific conditions.

High level protocol operations and functions are discussed in [13]. This document explains elementary concepts of LTE protocols such as scheduling, quality of service, handovers and power save operations. A comprehensive overview of physical layer basics and parameters is provided by ***J. Zyren, et al.*** [14]. Resource block configuration, physical channels and modulation schemes are also discussed in this research paper.

2.3 LTE Physical Downlink/Uplink Channel

Thomas A. Courtade, et al. [15] demonstrated optimal allocation of redundancy between packet-level erasure coding and physical-layer channel coding in fading channels. This

paper optimizes the allocation of redundancy between packet-level erasure coding (which provides additional packets to compensate for packet loss) and physical layer channel coding (which lowers the probability of packet loss). After some manipulation, standard optimization techniques determine the trade-off between the amount of packet-level erasure coding and physical-layer channel coding that minimizes the transmit power required to provide reliable communication. The results indicate that the optimal combination of packet-level erasure coding and physical-layer coding provides a significant benefit over pure physical-layer coding when no form of channel diversity is presented within a packet transmission. However, the benefit of including packet level erasure coding diminishes as more diversity becomes available within a packet transmission. Even with no diversity within a packet transmission, this paper shows that as the total redundancy becomes large the optimal redundancy for packet-level erasure coding reaches a limit while the optimal redundancy for physical-layer coding continues to increase. Hence providing limitless redundancy at the packet-level with rateless codes such as fountain codes is not the best use of limitless redundancy for block-fading channels.

Channel coding and decoding in a relay system operated with physical-layer network coding is proposed by ***Shengli Zhang, et al.*** [16]. This paper investigates link-by-link channel-coded PNC (Physical layer Network Coding), in which a critical process at the relay is to transform the superimposed channel-coded packets received from the two end nodes (plus noise). Specifically, this paper redesign the belief propagation decoding algorithm of the Repeat Accumulate (RA) code for traditional point-to-point channel to suit the need of the PNC multiple-access channel. Simulation results show that the new scheme outperforms the previously proposed schemes significantly in terms of Bit Error Rate (BER) without added complexity.

An interleaver is a critical component for the channel coding performance of turbo codes. Algebraic constructions are of particular interest because they admit analytical designs and simple, practical hardware implementations. Also, the recently proposed Quadratic Permutation Polynomial (QPP) based interleavers by Sun and Takeshita have provided excellent performance for short-to-medium block lengths, and have been selected for the 3GPP LTE standard. In his paper, author ***Eirik Rosnes*** [17] has demonstrated on the minimum distance of turbo codes with quadratic permutation polynomial interleavers. The computation of the best achievable minimum distances with QPP interleavers for all

3GPP LTE interleaver lengths N ≤ 4096 has been carried out and compares these minimum distances with the ones we get when using the 3GPP LTE polynomials.

Lanjun Liu, et al. [18] demonstrated the design and implementation of channel coding for underwater acoustic system. Underwater acoustic channel is a typical high bit error rate wireless channel. It is characterized by poor communication quality and high propagation delay. Based on comparing and analyzing the performances of Reed Solomon (RS) code, convolutional code, Turbo code, and RA code, a RA coding based underwater acoustic channel coding scheme is proposed in this paper. The results of Matlab based simulations show that the coding scheme can get a 100 times, or even more, performance improvement. In order to accelerate RA coding, aiming at the random mapping process of RA coding, based on the minimum sum algorithm, a lookup table based circuit design for fast iteration is introduced. Then, the experiments to test the RA coding are carried out in different channel environments, including underwater acoustic test platform and harbor. The results show that the coding scheme reduces the BER 38 times in the underwater acoustic test platform, increases the correct packet rate from 18.92% to 72.45% in the harbor.

Channel coding for single-user channels with rate-limited, coded, partial channel state information at the transmitter and full side information (SI) at the receiver is studied. Coding problems for channels with partial state information at the transmitter has demonstrated by ***Yakup Cemal, et al.*** [19]. Furthermore, special cases where the inner bound is tight are studied in this paper. Similarities between coding of SI as multiple partial descriptions and the multiple description problem of source coding theory are pointed out.

2.4 LTE Downlink/Uplink Channel Estimation

David Martin-Sacristan, et al. [20] demonstrated Medium Access Control (MAC) layer performance of different channel estimation techniques in UTRAN LTE Downlink. This paper uses an accurate LTE MAC layer simulator to perform a complete downlink LTE performance study. Results compare different channel estimation techniques showing significant difference among them, most of all regarding the robustness of the estimator against errors. Finally, LTE system performance assessment is presented employing a realistic channel estimator.

Fanghua Weng, et al. [21] demonstrated the channel estimation algorithms for the downlink of 3GPP LTE systems. By using computer simulation, the pilot signal assisted channel estimation algorithms based on least square (LS) and linear minimum mean square error (LMMSE) criteria, together with channel interpolation based on piecewise linear interpolation and DFT based interpolation are studied. By analyzing simulation results in terms of Mean Square Error (MSE) and uncoded BER, this paper concludes that the channel frequency responses of pilot tones are estimated by using LS estimator, and the channel frequency responses of data tones are interpolated by DFT based interpolation method is appropriate for the downlink of 3GPP LTE systems.

2.5 Source and Channel Coding for Wireless Media

Maria Fresia, et al. [22] has presented a general scheme for the lossy transmission of a source with arbitrary statistics through a noisy channel under the mean-square error fidelity criterion. This approach is based on transform coding, scalar quantization of the transform coefficients and linear encoding of the quantization indices. Entropy coding and channel coding are merged into a single linear encoding function, such that the catastrophic behaviour of conventional entropy coding is avoided and the full power of modern coding techniques and iterative “Belief-Propagation” decoding can be exploited. This approach is asymptotically optimal in the limit of large block length, for arbitrary source statistics and binary input-output symmetric channel.

Source and channel coding over multiuser channels in which receivers have access to correlated source side information are considered [23]. For several multiuser channel models necessary and sufficient conditions for optimal separation of the source and channel codes are obtained. In particular, the multiple-access channel, the compound multiple-access channel, the interference channel and the two-way channel with correlated sources and correlated receiver side information are considered and the optimality of separation is shown to hold for certain source and side information structures. Interestingly, the optimal separate source and channel codes identified for these models are not necessarily the optimal codes for the underlying source coding or the channel coding problems. In other words, while separation of the source and channel codes is optimal, the nature of these optimal codes is impacted by the joint design criterion.

2.6 LTE Performance Analysis

D. M. Sacristan, et al. [26], discussed some of the features of LTE such as MIMO, channel coding, and scheduling. Performance analysis in this paper is limited to downlink SISO and 2x2 MIMO scenarios. This paper mainly focuses on outlining the impact of different features of LTE on performance. However, at the time of this publication, some characteristics of LTE were under development, e.g., channel coding and rate matching, 4x4 MIMO. The impact of 2 antenna ports on spectral efficiency or the coding gain for 16-QAM and 64-QAM modulations by using turbo coding are demonstrated in this research paper.

In [25] the performance of single user MIMO (SU-MIMO) is studied with two multi stream MIMO schemes including Per Antenna Rate Control (PARC) and Pre-Coded MIMO (PREC) in two different simulation environment.

Both schemes can have four transmit and four receive antenna. It is concluded that the average sector throughput performance of the four stream scheme is 75-90% higher than the one with two stream schemes. Also, based on the comparison of two different four stream schemes (PARC 4x4 and PREC 4x4), PERC schemes seem to be better in average sector throughput gain (5-6%) and coverage gain (13-20%).

Performance study in [26] is limited to downlink transmission by using a MAC layer simulator. The main focus of this study is on evaluating the channel estimation method performance in Wiener low complexity (Wlc). Different estimation error impacts are investigated such as SNR estimation error, Doppler frequency estimation error, and PDP estimation error.

Simulation results are based on 10 MHz system bandwidth, one transmit and two receive antenna (SIMO). LTE downlink performance is evaluated based on the EVA channel and Wlc channel estimation method; however, high code rate and multi antenna schemes are not considered in performance analysis. The simulation is based on EVA channel and shows 5Mbps, 13 Mbps, and 31 Mbps of throughput for QPSK 1/3, 16 QAM ½ and 64QAM ¾ respectively. It is assumed that one antenna port is used.

The main technical features of LTE are presented by ***D.M. Sacristan, et al.*** [27], including MIMO, turbo coding used in LTE, and HARQ techniques. This paper also presents a performance analysis for 10 MHz of channel bandwidth, MIMO 4x4 and 2x2 in downlink and MIMO 1x2 in uplink cases. The downlink control channel overhead is assumed to be 2 OFDM symbols per subframe, and a 0.93 code rate is considered. Based

on these assumptions, the maximum throughput of the downlink and uplink is stated to be around 130 Mbps and 40 Mbps, respectively. This paper also includes an overview of the next LTE release (LTE-Advanced, release 10) which is under development.

In addition to conference and journal publications, 3GPP itself provides the maximum throughput of downlink and uplink as two report documents, [28] and [29] respectively. Reference [28] states the maximum throughput of downlink as 326.4 Mbps in the case of four antenna ports, one OFDM symbol assigned for Physical Downlink Control Channel (PDCCH), 20 MHz system bandwidth, 64-QAM modulation scheme and code rate of 1. Besides the code rate that is assumed to be 1, this calculation excludes reference signals and PDCCH. Also, [29] indicates that the maximum uplink throughput is 86.4 for 20 MHz system bandwidth, one transmit antenna, and 64-QAM modulation.

2.7 LTE characteristics and performance compared to other wireless communication standards

LTE is compared to WiMAX by ***A. Furuskar, et al.*** [30] with respect to spectrum efficiency, average user throughput, and cell edge bit rate gains for both TDD and FDD operations. Based on spectrum efficiency and average user throughput comparison, LTE outperforms WiMAX by about 60%. However, in uplink LTE is 100% better in cell edge and average performance.

Performance comparison of LTE and WiMAX by ***C. Ball, et al.*** [31] is based on Downlink FDD operation. This study compares the physical layer structure and gives the overhead for control channels for both standards. The results show better radio performance for LTE due to less overhead. The throughput calculation includes control and broadcast channel, however excludes the reference signal. In terms of SNR gain both standards have the same performance, but in respect to the throughput, LTE outperforms WiMAX [31].

By virtue of the crucial role of MIMO schemes in performance of wireless communication networks, MIMO technologies are compared for WiMAX, LTE and LTE-advanced by ***Q. Li, et al.*** [32]. In addition, ***Y. Yang, et al.*** [33] describes relay technologies for both communication standards and shows that by taking advantage of relay technologies, service coverage and system throughput is improved effectively.

2.8 Other LTE Topics

Considering the 3GPP evolution track, LTE-Advanced standardization is under development and the specifications and new technologies used in this version of 3GPP standards are discussed in some literature. In [34] a brief overview of Release 8 is provided, followed by LTE-Advanced requirements and technologies such as carrier aggregation, evolved MIMO schemes for uplink and downlink, etc. This article also provides peak spectral efficiency and radio access performance for uplink and downlink of LTE-Advanced. In [35] carrier aggregation, a critical technology used in LTE-Advanced that impacts the peak data rate and spectral efficiency is described in detail.

Different MU-MIMO schemes in Release 8 are verified in [36] by system level simulation and comparison to the zero-forcing technique of LTE-Advanced.

CHAPTER

3 PROPOSED CHANNEL ENCODING/DECODING MODEL FOR LTE-DL

3.1 Overview

In a mobile communication when a transmitter and receiver transmits and receives data and signal it uses channel. So, channel model is a crucial issue in all communication. A channel model is a set of rules or ways from which data or signal will smoothly sent or receive through the channel. A good channel model is essential for a high class of communication. A nice channel model could save bandwidth, signal power that increases the system capability.

In this chapter we introduce the proposed performance study model for channel coding and decoding for LTE. We will explain how this model works. In section 3.2 the channel coding and decoding model for LTE is outlined the principle of the proposed model is explained in subsequent sections.

Error control coding is a method to detect and possibly correct errors by introducing redundancy to the stream of bits to be sent to the channel. The Channel Encoder will add bits to the message bits to be transmitted systematically. After passing through the channel, the Channel decoder will detect and correct the errors. In general the channel encoder will divides the input message bits into blocks of k messages bits and replaces each k message bits block with a n-bit code word by introducing (n-k) check bits to each message block. Some major codes include the block codes, turbo codes and convolutional codes.

3.2 Channel Coding and Decoding Model for LTE Downlink

The model presented here has the following main blocks:

- Channel Coding Process
- Channel Decoding Process
- Additive White Gaussian Noise (AWGN)

- Hybrid Automatic Repeat Request (HARQ) Controller
- Throughput Measurement
- Dynamic Packing
- Delay
- Multiple input adder
- Limiter

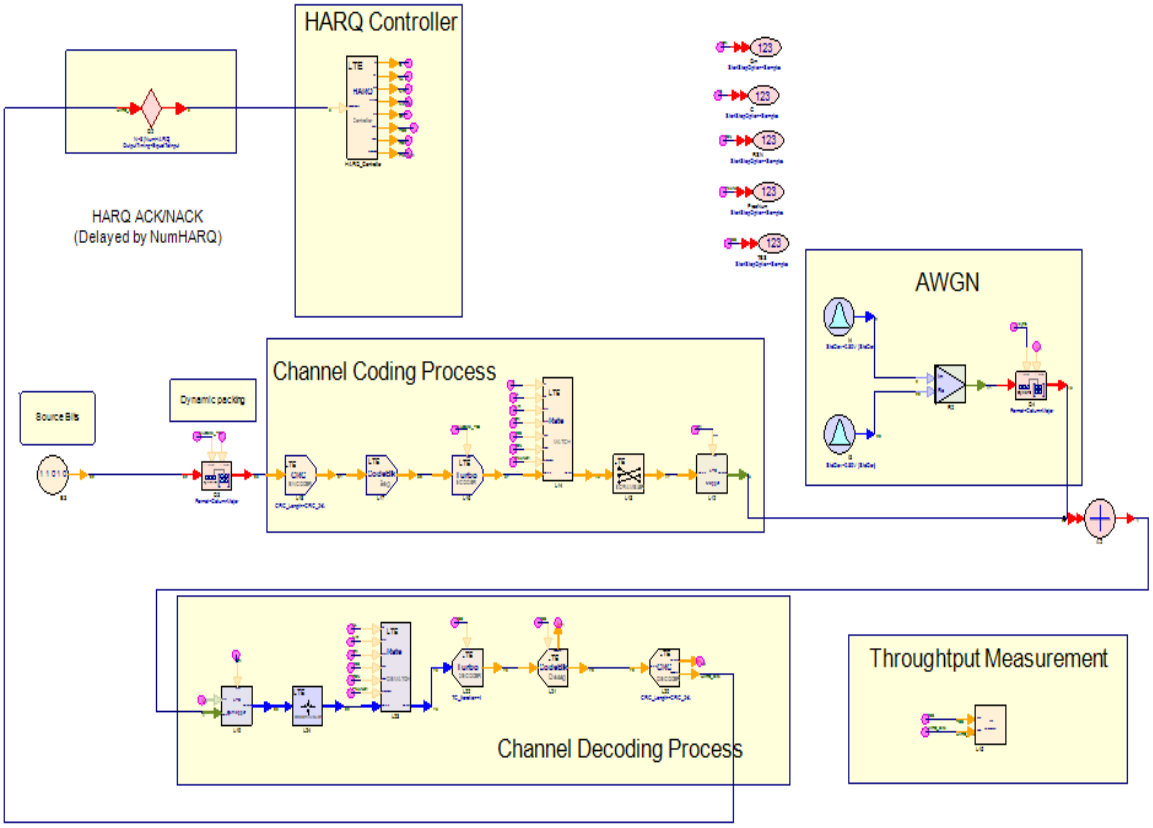

Figure 3.1: Channel coding and decoding model.

3.2.1 Channel coding process

In this section we explain the functioning of channel coding process.

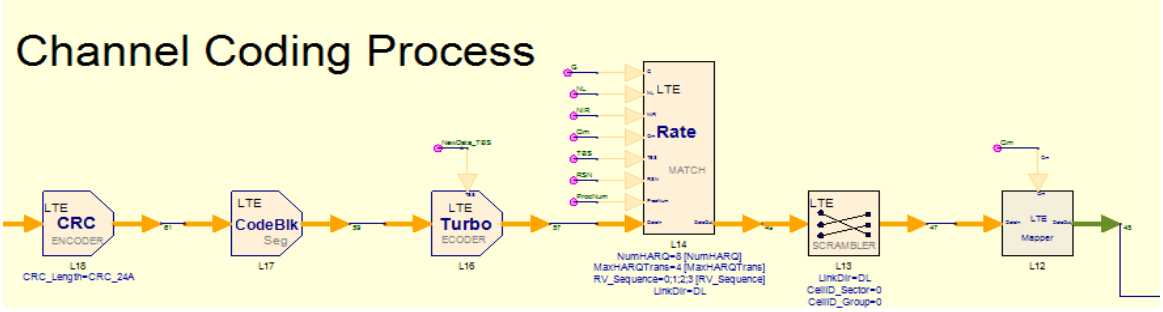

Figure 3.2: Channel coding process.

3.2.1.1 Random Bit Generator

This model generates a random bit sequence, in which the probability of a 0 bit is ProbofZero and the probability of a 1 bit is 1 - ProbofZero. The repeatability of the bit sequence generated by this model can be controlled by the Repeatable Random Sequences check box in the option tab of the dataflow analysis dialog.

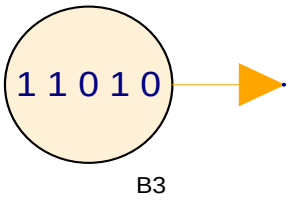

Figure 3.3: Random bit generator.

3.2.1.2 Dynamic Pack

Dynamic Pack packs variable numbers of input samples into output matrices based on numRows and numColumns control signals. A complete execution consists of two modes; control mode and operation mode. In control mode, Dynamic Pack reads one sample from numRows and one sample from numColumns, and the integer values specify number-of-rows and number-of-columns respectively for the matrix to be packed in the operation mode. In operation mode, Dynamic Pack reads (number-of-rows * number-of-columns) number of samples from input, then packs them into number-of-rows by number-of-columns output matrix in either column major or row major according to the Format parameter. If numRows is not connected, number-of-rows is default to be 1, which means a row vector. If numColumns is not connected, number-of-columns is default to be 1, which means a column vector. At least one of the control inputs (numRows, numColumns) must be connected.

The integer value for number-of-rows or number-of-columns can be 0 or negative, which results in an empty matrix.

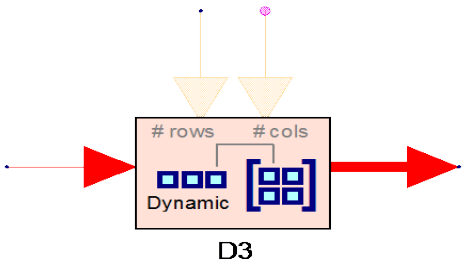

Figure 3.4: Dynamic Pack.

3.2.1.3 LTE Cyclic Redundancy Check (CRC) Encoder

This model is used to perform CRC attachment on LTE transport block. The input data for CRC calculation is divided by a polynomial, the remainder of this division is appended with input data. At the receiver side the received bits are divided by the same polynomial if the remainder is zero then the transmission was successful. If the result is not equal to zero, an error occurred during the transmission. In downlink two types of polynomials are used for CRC generation which is defined in 3GPP specification and given below.

$$g_{CRC24A}(D) = [D^{24} + D^{23} + D^{18} + D^{17} + D^{14} + D^{11} + D^{10} + D^{7} + D^{6} + D^{5} + D^{4} + D^{3} + D + 1] \quad (3.1)$$

$$g_{CRC24B}(D) = [D^{24} + D^{23} + D^{6} + D^{5} + D + 1] \text{ for a CRC length } L = 24 \quad (3.2)$$

CRC 24A is appended to the data, if data is divided in blocks then each block is also appended with CRC 24B. Code block segmentation is explained in next step.

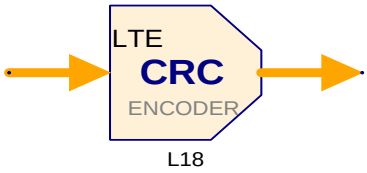

Figure 3.5: LTE CRC Encoder.

3.2.1.4 LTE Code Block Segmentation

This model is used to perform downlink/uplink transport block segmentation. Each firing, one matrix-based token is consumed in the DataIn port. The matrix vector size is denoted by B. One Matrix-based token is produced in the DataOut port. The matrix vector size is denoted by $C_+ * K_+ + C_- * K_-$. If the matrix size B at the DataIn port is equal to 0, nothing is done in this model and the matrix vector size at the DataOut port is also 0. The input bit vector sequence is denoted by $b_0, b_1, b_2,...,b_{B-1}$, where $B > 0$. If B is larger than the maximum code block size Z, segmentation of the input bit sequence is performed and an additional CRC sequence of $L = 24$ bits (using the CRC generator polynomial $g_{CRC24B}(D)$) is attached to each code block. The maximum code block size is $Z = 6144$. If the number of filler bits F calculated below is not 0, filler bits are added to the beginning of the first block. If $B < 40$, filler bits are added to the beginning of the code block. The filler bits are always set to NULL at the input of the encoder.

The bits output from code block segmentation are denoted by c_{r0}, c_{r1}, c_{r2}, c_{r3},...,$c_{r(Kr-1)}$, where r is the code block number, and K_r is the number of bits for code block r.

Number of bits in each code blocks (applicable for $C \neq 0$ only):

First segmentation size K_+ = minimum K such that $C \cdot K \geq B'$

if C = 1

the number of code blocks with length K_+ is $C_+ = 1$, $K_- = 0$, $C_- = 0$

else if C > 1

Second segmentation size K_- = maximum K such that $K < K_+$

$$\Delta_K = K_+ - K_-$$

Number of segments of size K_-: $C_- = \left\lfloor \frac{C.K_+ - B'}{\Delta_K} \right\rfloor$

Number of segments of size K_+: $C_+ = C - C_-$

end if

Number of filler bits $F = C_+ \cdot K_+ + C_- \cdot K_- - B'$

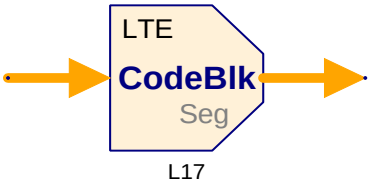

Figure 3.6: LTE code block segmentation.

3.2.1.5 LTE Turbo Encoder

This model is used to implement Turbo encoding for LTE downlink/uplink transport channel.

Each firing, if the TBS port is connected, one token is consumed in this port to get the transport block size (A). Otherwise, for the i^{th} firing, the element TransBlockSize [i % Size (TransBlockSize)] in the TransBlockSize parameter is read to get the transport block size (A). One matrix-based token is consumed in the DataIn port. The matrix vector size should be equal to $C_+ * K_+ + C_- * K_-$ given the transport block size (A). One Matrix-based token is consumed in the DataOut port. The matrix vector size is equal to $3*(C_+ * K_+ + C_- * K_) + C*12$ given the transport block size (A). The scheme of turbo coder is a Parallel Concatenated Convolutional Code (PCCC) with two 8-state constituent encoders and one turbo code internal interleaver. The coding rate of turbo coder is 1/3.

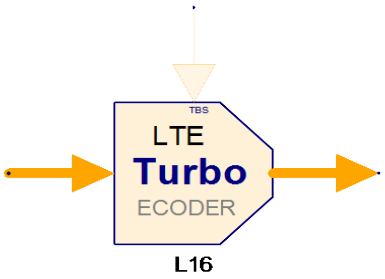

Figure 3.7: LTE turbo encoder.

3.2.1.6 LTE Rate Matching

This model is used to implement rate matching for turbo coded LTE Physical Downlink shared Channel (PDSCH)/Physical Uplink shared Channel (PUSCH). Each firing, one Matrix-based token is consumed in the DataIn port. The matrix vector size should be equal to $3*(C_+ * K_+ + C_- * K_-) + C*12$ given the transport block size (A).

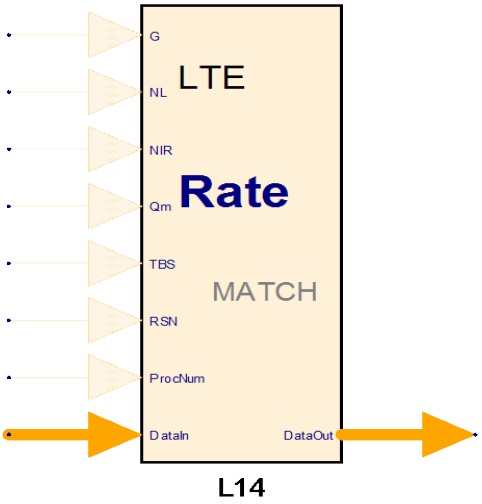

Figure 3.8: Rate Matching.

The other input ports could be connected or unconnected. If they are connected, one token is consumed each firing to get corresponding variable. If they are unconnected, the corresponding variable is gotten from input parameter. For the i^{th} firing, how to get the variable from input port or input parameter is shown in the following Table 3.1.

Table 3.1: Input parameter of rate matching.

Input Ports

Port	Name	Description	Signal Type	Optional
1	DataIn	Input Matrix-based data for rate matching	integer	NO
2	ProNum	Process number for each token at DataIn port	int	YES
3	RSN	Retransmission number for each token at the DataIn port	int	YES
4	TBS	Transport block size for each token at the DataIn port	int	YES
5	Qm	Modulation order for each token at the DataIn	int	YES
6	NIR	Soft buffer size for each token at the DataIn port, only for Downlink	int	YES
7	NL	Number of layers for each token at the DataIn port, only for Downlink	int	YES
8	G	Number of channel bits for each token at the DataIn port	int	YES

RSN = 0 means the first transport block transmission, RSN = 1 means the second transport block transmission (i.e. the first transport block retransmission), and so on. Modulation order table defines the mapping of MappingType (0: QPSK, 1: 16QAM, 2: 64QAM) and Modulation order (2: QPSK, 4: 16QAM, 6: 64QAM), shown in the table below.

Table 3.2: Modulation order table.

Value in the MappingType Parameter	Modulation order Qm
0	2 (QPSK)
1	4 (16QAM)
2	6 (64QAM)

The rate matching for turbo coded transport channels as shown below is defined per coded block and consists of interleaving the three information bit streams $d_k^{(0)}$, $d_k^{(1)}$ and $d_k^{(2)}$, followed by the collection of bits and the generation of a

circular buffer as depicted in the following Fig. 3.9. The output bits for each code block are transmitted.

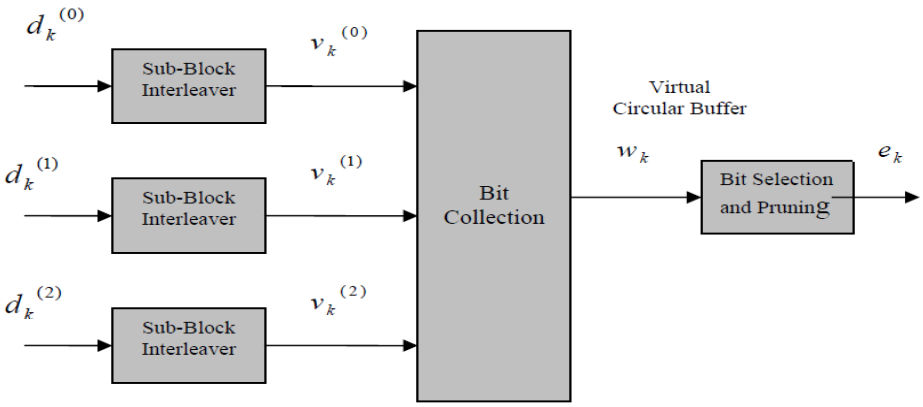

Figure 3.9: Internal block diagram of rate matching.

It should be noted that if the ProcNum port is connected, the input ProcNum should start with 0, then 1, 2,...., NumHARQ - 1, 0, 1,.... One exception is that ProcNum = -1 is allowed which means no transmission is allocated in this firing, and could be in any position of input sequence. For example, NumHARQ = 4, the input ProcNum sequence could be 0, -1, 1, 2, 3, -1, -1, 0, 1, 2, -1, 3.

3.2.1.7 LTE Downlink and Uplink Scrambler

This model is used to perform scrambling for PDSCH/PUSCH. Each firing, one Matrix-based token is consumed in the DataIn port. The matrix vector size is denoted by M_{bit}. One Matrix-based token is produced in the DataOut port. The matrix vector size is also denoted by M_{bit}. The mapping of subframe index and firing index is shown as SubframeIndex = FiringIndex % 10, where 10 is the number of subframes in one radio frame. In uplink, the block of bits b(0),....,b(M_{bit}-1), where M_{bit} is the number of bits transmitted on the physical uplink shared channel in one subframe, shall be scrambled with a UE specific scrambling sequence prior to modulation, resulting in a block of scrambled bits $\tilde{b}(0)$,...., $\tilde{b}(M_{bit} - 1)$ according to pseudo code. M_{bit} is the sum of number of channel bits for PUSCH data and coded bits of CQI/PMI and RI. It is required that the x and y bits should be set to -1 and -2 respectively.

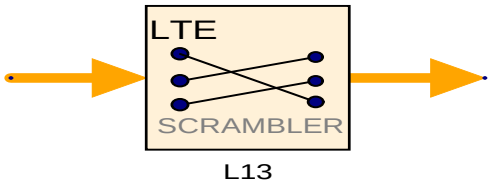

Figure 3.10: LTE UP/DL Scrambler.

In downlink, For each code word q, the block of bits $b^{(q)}(0),...,b^{(q)}(M_{bits}^{(q)} - 1)$, where $M_{bits}^{(q)}$ is the number of bits in code word q transmitted on the physical channel in one subframe, shall be scrambled prior to modulation, resulting in a block of scrambled bits $\tilde{b}(0),...., \tilde{b}(M_{bit} - 1)$. Up to two code words can be transmitted in one subframe, i.e., $q \in \{0, 1\}$. In the case of single code word transmission, q is equal to zero. $M_{bit}^{(q)}$ equals the number of channel bits for PDSCH of this codeword.

3.2.1.8 LTE Mapper

This model takes binary digits, 0 or 1, as input and produces complex valued modulation symbols, x = I + jQ, as output. Each firing, one Matrix-based token is consumed at the DataIn pin. The matrix vector size is denoted by M_{bit}.

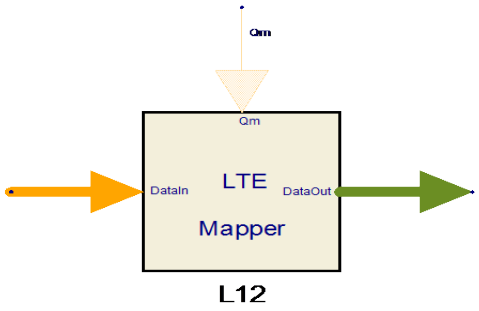

Figure 3.11: LTE Mapper.

If the Qm pin is connected, one token is consumed each firing to get the modulation order Qm (2: QPSK, 4: 16QAM, 6: 64QAM). Otherwise, for the i^{th} firing, the element MappingType [i % Size (MappingType)] in the MappingType parameter is read to get the modulation order Qm. The mapping of the value in the MappingType parameter and the modulation order Qm is shown above in the Table 3.2. One Matrix-based token is produced at the DataOut pin. The matrix vector size, denoted by M_{symb}, is M_{bit}/Qm. When Qm equals to 2, QPSK mapping is used. When Qm equals to 4, 16QAM mapping is used. When Qm equals to 6, 64QAM mapping is used.

QPSK mapping: In case of QPSK modulation, pairs of bits, b(n) b(n+1), are mapped to complex-valued modulation symbols x = I + jQ according to the QPSK Modulation Mapping table.

Table 3.3: QPSK Mapping.

b(n), b(n+1)	I	Q
00	$1/\sqrt{2}$	$1/\sqrt{2}$
01	$1/\sqrt{2}$	$-1/\sqrt{2}$
10	$-1/\sqrt{2}$	$1/\sqrt{2}$
11	$-1/\sqrt{2}$	$-1/\sqrt{2}$

16QAM mapping: In case of 16QAM modulation, pairs of bits, b(n) b(n+1) b(n+2) b(n+3), are mapped to complex-valued modulation symbols x = I + jQ according to the 16QAM Modulation Mapping similar to the QPSK mapping table except number of variables.

64QAM mapping: In case of QPSK modulation, pairs of bits, b(n) b(n+1) b(n+2) b(n+3) b(n+4) b(n+5), are mapped to complex-valued modulation symbols x = I + jQ according to the 64QAM Modulation Mapping.

3.2.2 Multiple Input Adder

The Add model produces the sum of the inputs at the output. This model reads 1 sample from all inputs and writes 1 sample to the output. In the present channel coding model it adds the coded output and the white Gaussian noise during transmission. For a single input add, the input is copied to the output.

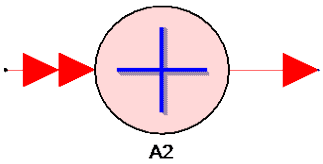

Figure 3.12: Multiple input adder.

3.2.3 Additive White Gaussian Noise (AWGN)

The additive white Gaussian channel model is the one of the simplest channel model in wireless communication. It is very simple because a white noise is only added with the wireless channel. In additive white noise a specific and equal amount of noise is added in

every frequency spectrum. The AWGN channel model does not consider any fading effect, Inter-symbol interference that's why it is very simple and straight forward. It is a simple mathematical model it only consider the thermal noise and short noise.

3.2.3.1 Gaussian Noise Waveform

This model generates a Gaussian noise waveform which is Identically independently distributed varieties with Gaussian distribution as specified by mean from the Offset parameter and standard deviation from the StdDev parameter are output. The output is commonly referenced as additive white Gaussian noise (AWGN).

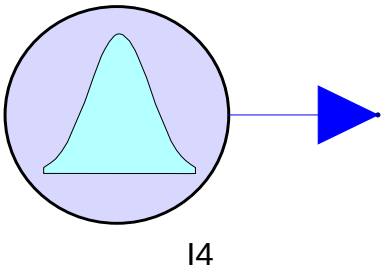

Figure 3.13: Gaussian noise waveform.

3.2.3.2 Real and Imaginary to Complex Converter (RectToCx)

The RectToCx model converts input real and imaginary values to output complex values. This model reads 1 sample from the inputs real and imaginary and writes 1 sample to the output.

$$\text{Output} = \text{real} + j \times \text{imaginary}$$

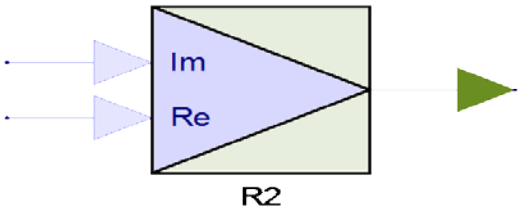

Figure 3.14: Real and Imaginary to complex converter.

3.2.4 Channel Decoding Process

Channel decoding is the opposite process of channel coding. The functional blocks of channel decoding process are explained below.

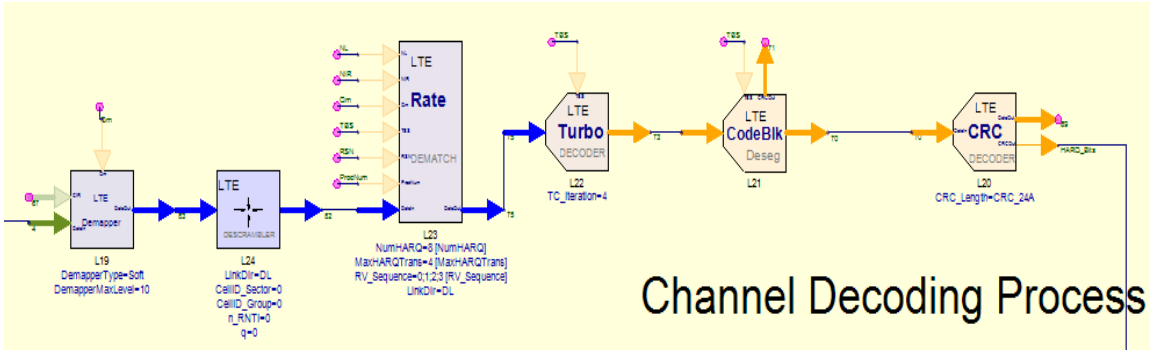

Figure 3.15: Channel decoding process.

3.2.4.1 LTE Demapper

This model demaps uniform QPSK, 16QAM and 64QAM to bits used for channel decoding. Each firing, one Matrix-based token is consumed at the DataIn pin. The matrix vector size is denoted by M_{symb}. If the Qm pin is connected, one token is consumed each firing to get the modulation order Qm (2: QPSK, 4: 16QAM, 6: 64QAM). Otherwise, for the i^{th} firing, the element Mapping Type [i % Size (Mapping Type)] in the Mapping Type parameter is read to get the modulation order Qm.

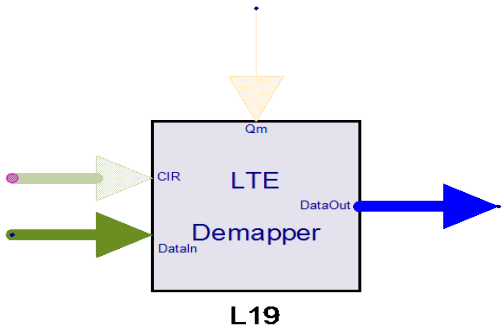

Figure 3.16: LTE demapper.

3.2.4.2 LTE Downlink and Uplink Descrambler

This model is used to perform descrambling for PDSCH/PUSCH. The SubframeIgnored parameter specifies the number of subframes that are ignored at the beginning due to the receiver delay. For a typical LTE receiver in this library for closed-loop HARQ transmission, one subframe delay is introduced in the receiver. In this case the first subframe is ignored in the subframe indexing below. Each firing, one Matrix-based token is consumed in the DataIn port. The matrix vector size is denoted by M_{bit}. One Matrix-based token is produced in the DataOut port. The matrix vector size is also denoted by M_{bit}. The mapping of subframe index and firing index is shown as

SubframeIndex = FiringIndex % 10, where 10 is the number of subframes in one radio frame. Note that the first SubframeIgnored firings are excluded in the firing indexing. For the benefit of soft decision decoding of Turbo codes, this model supports descrambling for soft information.

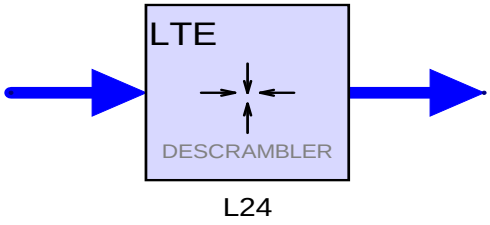

Figure 3.17: LTE downlink and uplink descrambler.

3.2.4.3 LTE Downlink and Uplink Rate Dematching

This model implements the inverse operation of LTE Rate Matching. This model is used to implement rate dematching for LTE PDSCH/PUSCH. The SubframeIgnored parameter specifies the number of subframes that are ignored at the beginning due to the receiver delay. For a typical LTE receiver in this library for closed loop HARQ transmission, one subframe delay is introduced in the receiver. In this case the first subframe is ignored in the subfram indexing below. Each firing, one Matrix-based token is consumed in the DataIn port. The matrix vector size should be equal to the number of channel bits (G). The other input ports could be connected or unconnected. If they are connected, one token is consumed each firing to get corresponding variable. If they are unconnected, the corresponding variable is gotten from input parameter. For the i^{th} firing, how to get the variable from input port or input parameter is shown in the following table.

Table 3.4: Parameters of Rate dematching.

Variable	**Port (if port is connected)**	**Parameter (if port is unconnected)**
Process number (ProcNum)	ProcNum	N/A
Retransmission number (RSN)	RSN	N/A
Transport Block Size (A)	TBS	TransBlock
Modulation order (Qm)	QM	ModulationOrderTable
Soft buffer size (N_{IR})	NIR	Nir
Number of layers (NL)	NL	NumOfLayers

RSN = 0 means the first transport block transmission, RSN = 1 means the second transport block transmission (i.e. the first transport block retransmission), and so on. Modulation order table defines the mapping of Mapping Type (0: QPSK, 1: 16QAM, 2: 64QAM) and Modulation order (2: QPSK, 4: 16QAM, 6: 64QAM), shown in the Table 3.2.

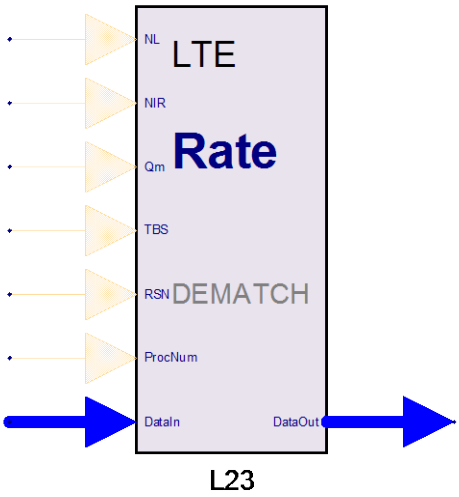

Figure 3.18: LTE downlink and uplink rate dematching.

3.2.4.4 LTE Turbo Decoder

This model is used to implement Turbo decoding for LTE downlink/uplink transport channel. Each firing, if the TBS port is connected, one token is consumed in this port to get the transport block size (A). Otherwise, for the i^{th} firing, the element TransBlockSize [i % Size (TransBlockSize)] in the TransBlockSize parameter is read to get the transport block size (A). One Matrix-based token is consumed in the DataIn port. The matrix vector size should be equal to $3*(C_+ * K_+ + C_- * K_-) + C*12$ given the transport block size (A). One Matrix-based token is consumed in the DataOut port. The matrix vector size is equal to $C_+ * K_+ + C_- * K_-$ given the transport block size (A). An iterative decoding scheme based on the modified Berrou et al. algorithm is used in this model. The iterative number can be set from 1 through to 20 through the TC_Iteration parameter. In theory, as the number of these iterations approaches infinity, the estimate at the output of decoder will approach the maximum a posterior (MAP) solution. The following figure shows the Turbo decoder structure.

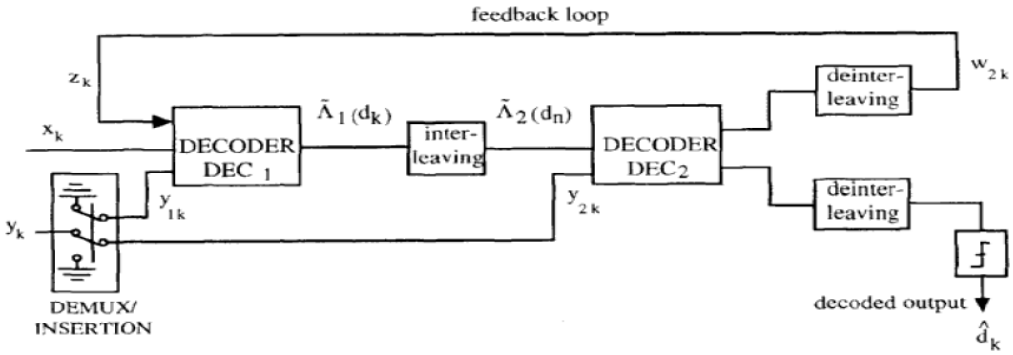

Figure 3.19: LTE Turbo decoding structure.

Decoder 1 computes Logarithm of Likelihood Ration (LLR) associated with each decoded bit from the systematic information (X_k), redundant information of encoder 1 (y_{1k}) and extrinsic information (Z_k).

Decoder 2 takes as input the interleaved version of LLR, the redundant information of second encoder (y_{2k}). The extrinsic information from decoder 2 is interleaved to produce Z_k, which is fed back to decoder 1. Note that, when it is determined by the Turbo decoder that the input sequence cannot be decoded, a fixed sequence (10101010...) is output.

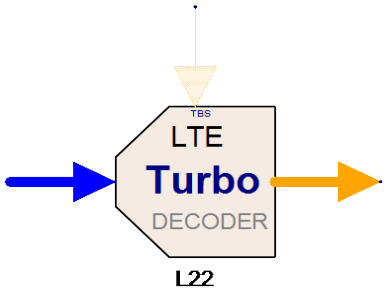

Figure 3.20: LTE Turbo decoder.

3.2.4.5 LTE Code Block Desegmentation

This model is used to perform the code block desegmentation on the input bit sequence. Each firing, if the TBS port is connected, one token is consumed in this port to get the transport block size (A). Otherwise, for the i^{th} firing, the element TransBlockSize [i % Size (TransBlockSize)] in the TransBlockSize parameter is read to get the transport block size (A). One Matrix-based token is consumed in the DataIn port. The matrix vector size should be equal to $C_+ * K_+ + C_- * K_-$ given the transport block size (A). One Matrix-based token is produced in the DataOut port. The matrix vector size is denoted by B, where B = A + L (L = 24 for CRC length). One Matrix-based token is produced in the CRCOut port.

The matrix vector size is equal to C if C > 1, or equal to 0 if C = 1. When C > 1, the CRC check result for each code block is output in this port, where 1 means CRC check success, 0 means CRC check failure. The input bits to the code block desegmentation are denoted by c_{r0}, c_{r1}, c_{r2}, c_{r3},..., $c_{r(Kr-1)}$, where r is the code block number, and K_r is the number of bits for code block r.

Number of bits in each code blocks (applicable for $C \neq 0$ only):

First segmentation size K_+ = minimum K such that $C \cdot K \geq B'$

if C =1

the number of code blocks with length K_+ is $C_+ = 1$, $K_- = 0$, $C_- = 0$

else if C > 1

Second segmentation size K_- = maximum K such that $K < K_+$

$$\Delta_K = K_+ - K_-$$

Number of segments of size K_-: $C_- = \left\lfloor \frac{C.K_+ - B'}{\Delta_K} \right\rfloor$

Number of segments of size K_+: $C_+ = C - C_-$

end if

Number of filler bits $F = C_+ \cdot K_+ + C_- \cdot K_- - B'$

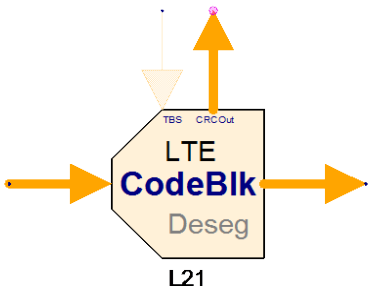

Figure 3.21: LTE code block desegmentation.

3.2.4.6 LTE CRC Decoder

This model is used to perform CRC decoding on coded LTE transport block. Each firing, one Matrix-based token is consumed in the DataIn port. The matrix vector size is denoted by B, where B > L, where L is CRC length depending on the CRC_Length parameter shown in the table below. One Matrix-based token is produced in the DataOut port. The matrix vector size is denoted by A, where A = B - L. One token is produced in the CRCOut port, indicating the CRC check result, where 1 means CRC check success, 0 means CRC check failure. The matrix vector size is 1. Note that if the matrix size at the

DataIn port is equal to 0, nothing is done in this model and the matrix vector size at the DataOut port is also 0. The parity bits are generated by cyclic generator polynomials given in section 3.1.1.3.

Each firing, this model performs CRC encoding on the first A tokens of the input sequence and gets L parity tokens, which will be compared with the last L tokens of input sequence. If the result is the same, 1 is output at CRCOut, otherwise 0 is output at CRCOut.

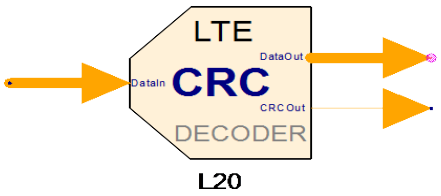

Figure 3.22: LTE CRC decoder.

3.3 Delay

The Delay model introduces a delay of N samples to the input signal. For every input, there is one output. The initial N output samples have a null value. For scalar signals, a null value is 0. For matrix signals, a null value is a matrix with the same size as the input matrix and with all its elements set to 0.

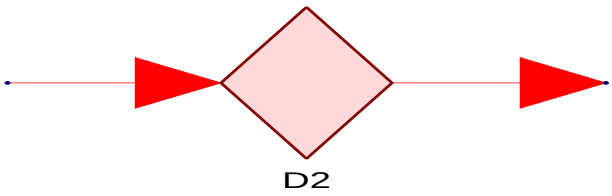

Figure 3.23: Delay.

3.4 LTE Hybrid Automatic Repeat Request (HARQ) Controller

This model is used to control HARQ transmission for downlink/uplink transport channels, by inputting HARQ Acknowledge/No-acknowledge (ACK/NACK) which is feedbacked from receiver and outputting corresponding control signals. LTE closed-loop HARQ simulation employs dynamic data flow.

Each firing, one token is consumed at the HARQ_Bits port, where 1 indicates CRC check success, 0 indicates CRC check failure. When HARQ_Enable is set NO, this port could

be unconnected and no data is read from this port; when HARQ_Enable is set YES, the data is read from this port when this port is connected, and the value '1' (HARQ ACK) is assumed when this port is unconnected.

One token is produced at the ProcNum port, indicating the process number for this subframe. When this subframe is not allocated with transport channel, -1 is output.

Table 3.5: Input port parameters of HARQ controller.

Input Port

Port	Name	Description	Signal Type	Optional
1	HARQ_Bits	HARQ ACK/NACK bits feedbacked from the receiver	Int	YES

Table 3.6: Output port parameters of HARQ controller.

Output Port

Port	Name	Description	Signal Type	Optional
1	ProcNum	Process number for each subframe	int	NO
2	RSN	Retransmission number for each subframe	int	NO
3	TBS	Transport block size for each subframe	int	NO
4	Qm	Modulation order for each subframe	int	NO
5	M_{symb}	Number of modulation symbols for each subframe		NO
6	NIR	Soft buffer size for each subframe, only for Downlink	int	NO
7	NL	Number of layers for each subframe, only for Downlink	int	NO
8	G	Number of channel bits for each subframe	int	NO

One token is produced at the RSN port, indicating the retransmission number for this subframe, only valid when ProNum is not equal to -1. RSN = 0 means transmission of new transport block. One token is produced at the TBS port, indicating the transport block size for this subframe, only valid when ProNum is not equal to -1. One token is produced at the Qm port, indicating the modulation order for this subframe, only valid when ProNum is not equal to -1. One token is produced at the Msymb port, indicating the number of modulation symbols for this subframe, only valid when ProNum is not equal

to -1. One token is produced at the NIR port, indicating the soft buffer size for this subframe, only valid when ProNum is not equal to -1 and when downlink is set. One token is produced at the NL port, indicating the transport block size for this subframe, only valid when ProNum is not equal to -1 and when downlink is set. One token is produced at the G port, indicating the number of channel bits for this subframe, only valid when ProNum is not equal to -1.

The SubframeIgnored parameter specifies the number of subframes that are ignored at the beginning due to the receiver delay. For a typical LTE receiver in this library for closed-loop HARQ transmission, one subframe delay is introduced in the receiver. In this case the first subframe is ignored in the subframe indexing below. For the first SubframeIgnored subframe, the output at the ProNum Port are -1 indicating no valid process is allocated in these subframes.

The output values at the Qm, Msymb, NIR, NL and G ports are related to the subframe index (firing index). For the i^{th} firing excluding the first SubframeIgnored firings, the output values at the port above are the corresponding setting in this i % 10 subframe, where 10 indicates the number of subframes in one radio frame.

In LTE, some subframes may be not allocated for HARQ transmission.

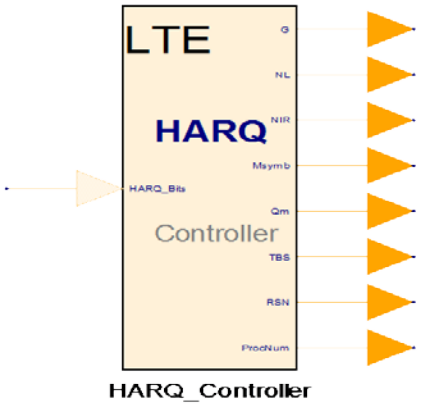

Figure 3.24: HARQ controller.

The followings shows the cases that subframes are not allocated for HARQ transmission.

In TDD mode

- The non-active subframes that are allocated to uplink when downlink signal is simulated.

- The non-active subframes that are allocated to downlink when uplink signal is simulated.

In FDD mode

- No transport block is allocted in the subframes (even when a number of resouce blocks (RBs) are allocated).

3.5 LTE Throughput Measurement

This model performs the averaged closed-loop HARQ throughput over subframes from Subframe Start to Subframe Stop for both PDSCH and PUSCH.

Each firing, one token is consumed at both 'TBS' port and 'CRCParity' port. The data input from the 'TBS' port indicates the transport block size for each subframe. If the input value at this port is '0', it is assumed that no transport block is allocated in this subframe. This occurs in TDD mode or when the transport block size for one specific subframe is set to '0' manually by users. The data input from the 'CRCParity' port is the CRC check result for each subframe, where '1' means CRC check is successful and '0' means CRC check fails.

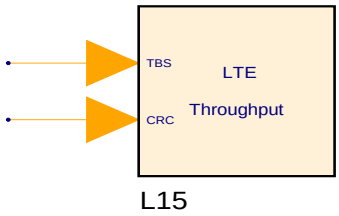

Figure 3.25: LTE throughput measurement.

If this model is used in the scenario that the LTE receiver is delayed by one subframe, the throughput calculation should at least start from the second subframe (SubframeStart >= 1).

The calculated results that are output to the data set are shown below.

- Throughput(averaged throughput (bps) over specified subframes): The calculation equation is

$$\text{Throughput} = \sum_{Subframe\ Start}^{Subframe\ Stop} TBS * CRCParity * 1000 \qquad (3.3)$$

where 1000 is the reciprocal of 1 msec.

- ThroughtputFraction (the fraction (%) of averaged throughput to the maximum possible throughput): The calculation equation is

$$\text{ThroughputFraction} = \frac{\sum_{Subframe\ \ Start}^{Subframe\ \ Stop} TBS * CRCParity}{\sum_{Subframe\ \ Start}^{Subframe\ \ Stop} TBS} \tag{3.4}$$

- Block Error Rate(BLER): The calculation equation is

$$\text{BLER} = \frac{\sum_{Subframe\ \ Start}^{Subframe\ \ Stop} (1 - CRCParity)}{\sum_{Subframe\ \ Start}^{Subframe\ \ Stop} (1)} \tag{3.5}$$

CHAPTER

4

SMULATION RESULTS AND ANALYSIS

4.1 Simulation Results

In this chapter the results of the simulation are illustrated and discussed. The 3GPP LTE channel coding and decoding model described in chapter 3 has been simulated using SystemVue software. The channel mode is assumed to be AWGN and normal cyclic prefix is used. The LTE turbo code basic code rate is 1/3 and supported modulation schemes are Quadrature Phase Shift Keying (QPSK), 16QAM and 64QAM. The bandwidth is 5 MHz for the simulation, using all 300 sub carriers. A normal cyclic prefix of length is inserted among data to cancel the effect of multipath channel to remove ISI. In simulating the Single Input Single Output (SISO) system, only one port of an antenna is considered and this antenna port is treated as physical antenna. The performance of the system is measured by measuring the throughput and Block Error Rate (BLER). The designed simulator is flexible to use, there is option to use bandwidth from 1.4 to 20 MHz. Other simulation parameters are described and summarized in following Table 4.1.

Table 4.1: Simulation Parameters.

Parameter	Value(s)
System Bandwidth	5 MHz
Modulation Format	QPSK, 16QAM, 64QAM
Frame Period	10 ms
Subcarrier spacing	15 KHz
Cyclic prefix	Normal
Duplex mode	FDD
Maximum number of RBs	25
Antenna diversity	Single input port
Number of subcarriers per PRB	12

Fig. 4.1 demonstrates FDD downlink throughput in bps values versus SNR for single antenna port and 5 MHz of system bandwidth in QPSK modulation scheme. It is shown that the throughput increases with the SNR. The maximum throughput in 5 MHz of system bandwidth and single antenna port is 2.173 Mbps and minimum is 1.049 Mbps. The results of Fig. 4.1 are summarized in Table 4.2.

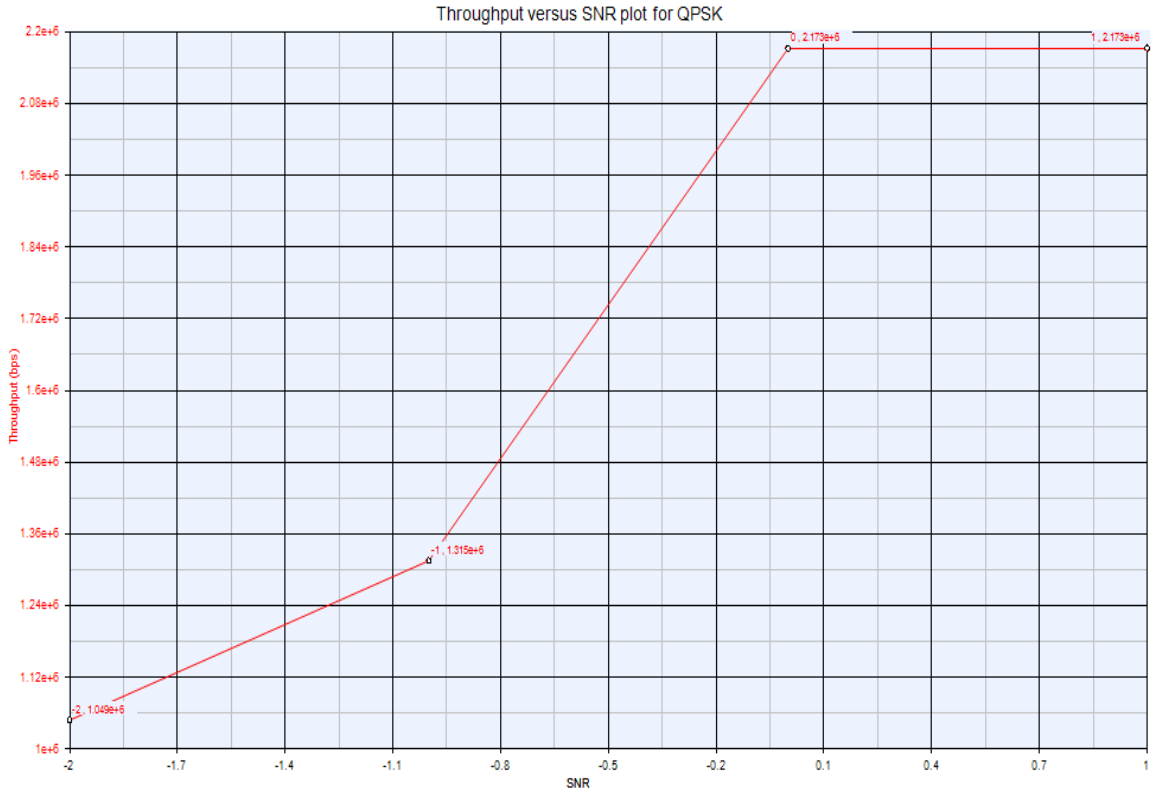

Figure 4.1: Throughput v/s SNR plot for QPSK.

Now we have a Table 4.2, shown below depicts the variations of throughput with SNR.

Table 4.2: Throughput and SNR simulation results for QPSK.

SNR	**Throughput (Mbps)**
-2	1.049
-1.4	1.06
-0.8	1.837
-0.2	2.173
0.4	2.173
1	2.173

In the above section we have analysed the simulated results for throughput, now Fig. 4.2 demonstrates FDD downlink throughput Fraction (throughput in percentage) values versus SNR for single antenna port and 5 MHz of system bandwidth in QPSK modulation scheme. It is shown that the throughput increases with SNR. The maximum throughput in 5 MHz of system bandwidth and one antenna port is 100% and minimum is 48.226%.

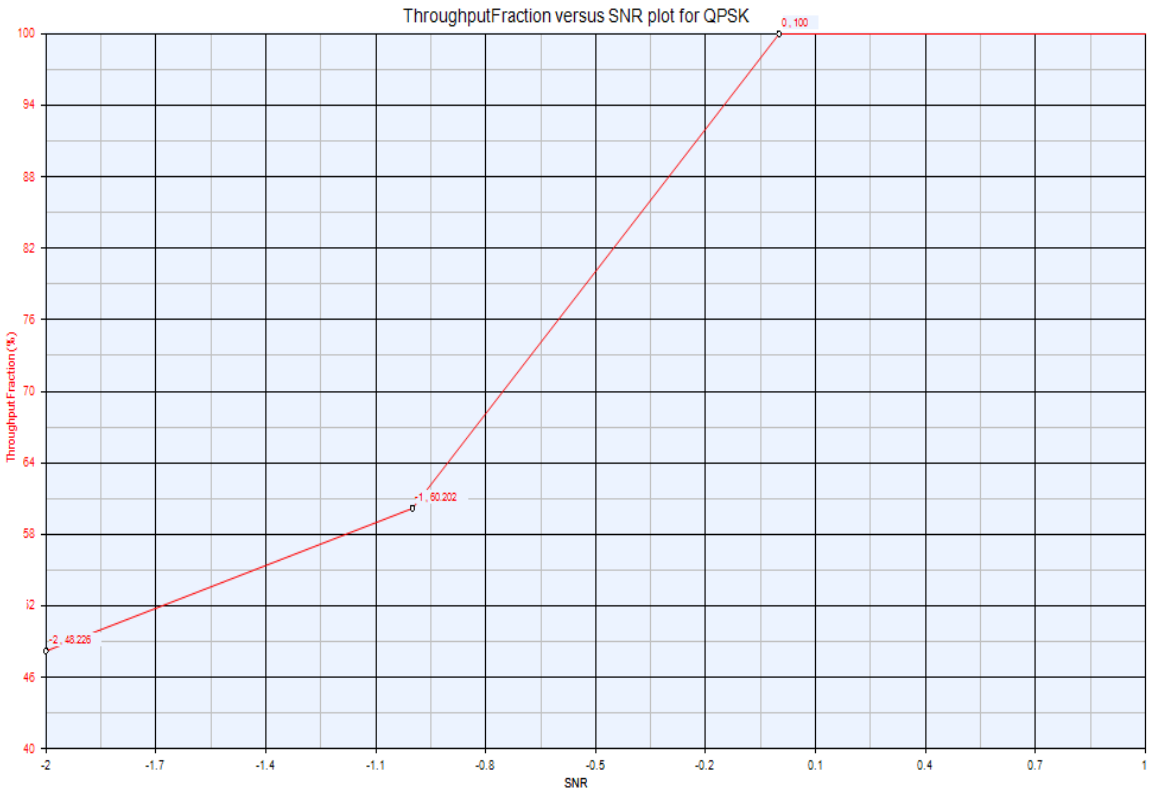

Figure 4.2: Throughput Fraction v/s SNR plot for QPSK.

The results of Fig. 4.2 are summarized in Table 4.3.

Table 4.3: Throughput Fraction and SNR simulation results for QPSK.

SNR	**Throughput Fraction (%)**
-2	48.226
-1.4	48.733
-0.8	84.474
-0.2	100
0.4	100
1	100

Block Error Rate (BLER) is also an important parameter to measure the performance of communication system, hence in this section the BLER values versus SNR analysis for QPSK modulation scheme is demonstrated. Fig. 4.3 shows the simulated graph for BLER versus SNR.

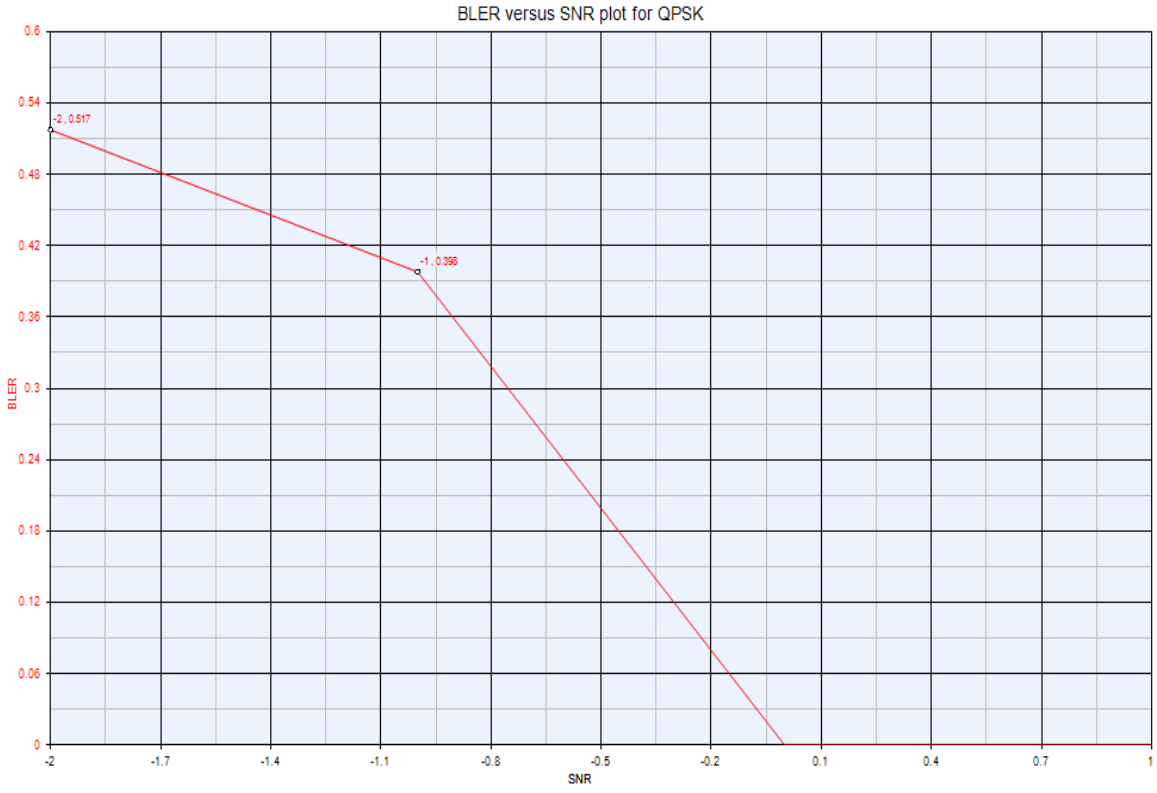

Figure 4.3: Block Error Rate (BLER) v/s SNR plot for QPSK.

Fig. 4.3 shows the performance measured in terms of BLER versus SNR. As we know that BLER is also an important parameter to measure the performance.

Table 4.4: BLER and SNR simulation results for QPSK.

SNR	**Block Error Rate (BLER)**
-2	0.517
-1.4	0.512
-0.8	0.154
-0.2	0
0.4	0
1	0

Above figure shows as the SNR increases the BLER decreases which means the performance of the system increases the maximum value of BLER is 0.517 and minimum is 0. Table 4.4 summarises the results of Fig. 4.3.

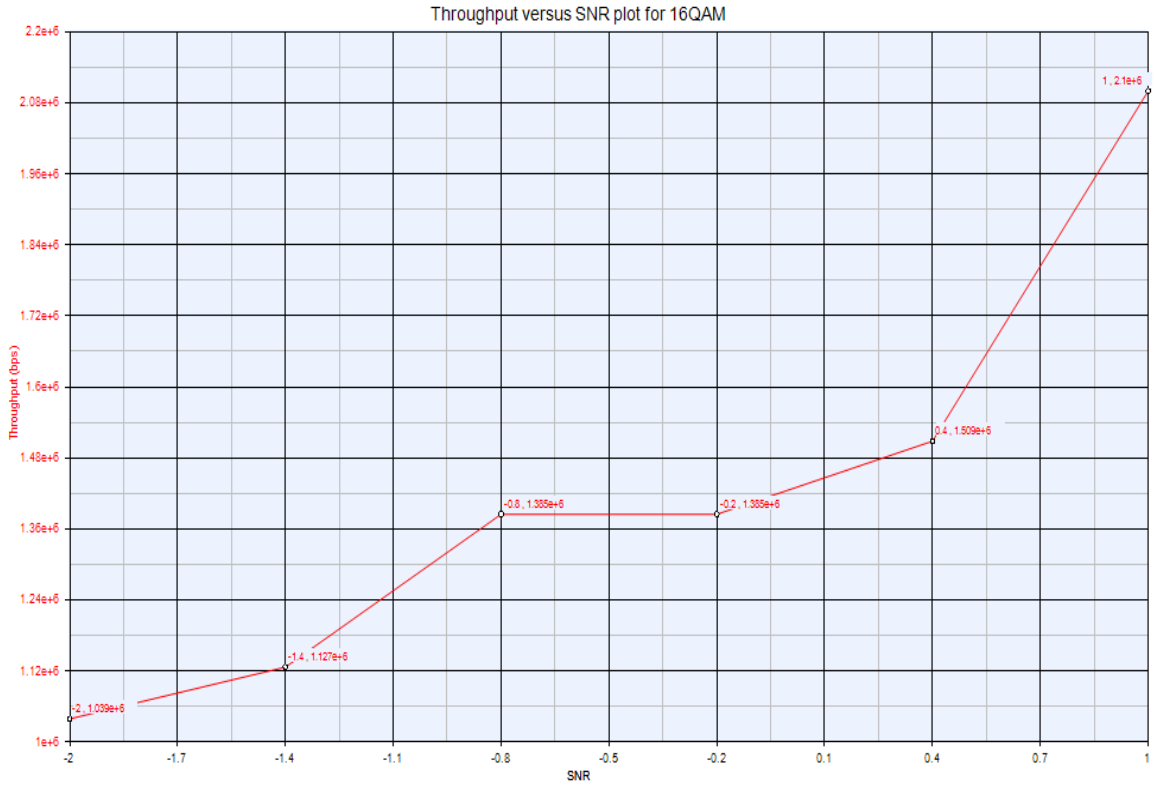

Figure 4.4: Throughput v/s SNR plot for 16QAM.

Table 4.5: Throughput and SNR simulation results for 16QAM.

SNR	**Throughput (Mbps)**
-2	1.039
-1.4	1.127
-0.8	1.385
-0.2	1.385
0.4	1.509
1	2.1

From Fig. 4.4 and Table 4.5 it is inferred that the system performance degrades using 16QAM. The maximum value of the throughput using 16QAM is

Mbps at 5 MHz bandwidth. It is shown that the throughput increases with the SNR. The maximum throughput in 5 MHz of system bandwidth and one antenna port is 2.1 Mbps and minimum is 1.039 Mbps. The results of Fig. 4.4 are summarized in Table 4.5.

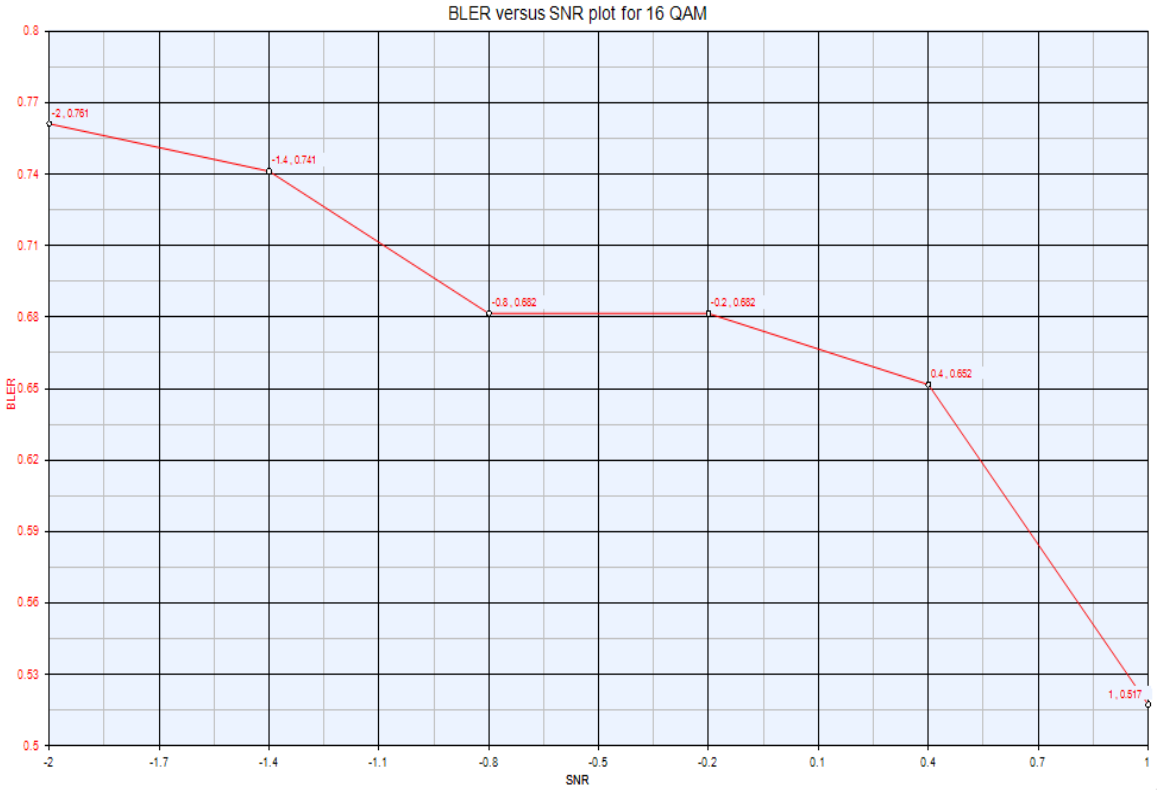

Figure 4.5: Block Error Rate (BLER) v/s SNR plot for 16QAM.

Table 4.6: BLER and SNR simulation results for 16 QAM.

SNR	**Block Error Rate (BLER)**
-2	0.761
-1.4	0.741
-0.8	0.682
-0.2	0.682
0.4	0.652
1	0.517

From Fig. 4.5 and Table 4.6 it is inferred that the system performance degrades using 16QAM. Block Error Rate (BLER) is an important parameter to measure the performance of communication system, hence in this section the BLER values versus SNR analysis for 16QAM modulation scheme is demonstrated. Fig. 4.5 shows the simulated graph for

BLER versus SNR, for the better performance of the communication system BLER should be mitigated. It is clear from the simulated results that the QPSK performance is much better than the 16QAM. In case of the QPSK the value of the BLER becomes zero at SNR equals to 1, while for the 16QAM it is 0.517.

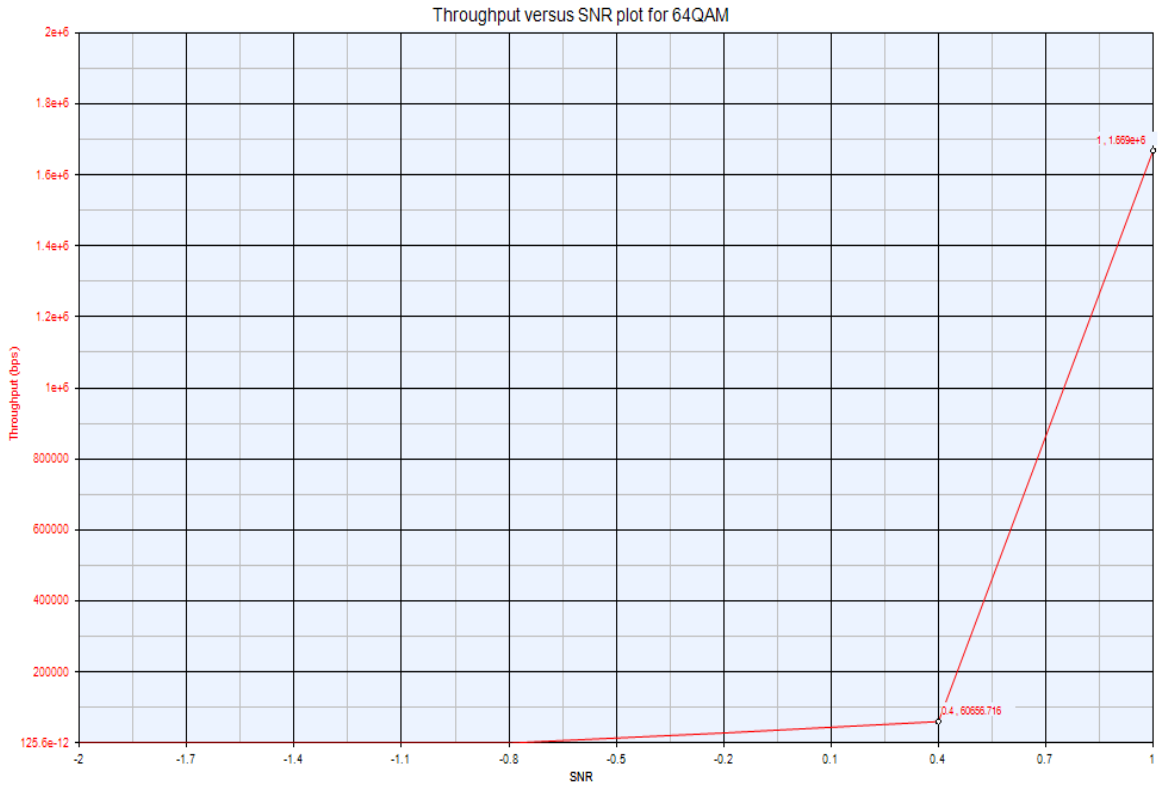

Figure 4.6: Throughput v/s SNR plot for 64 QAM.

Table 4.7: Throughput and SNR simulation results for 64QAM.

SNR	**Throughput (Mbps)**
-2	0
-1.4	0
-0.8	0
-0.2	0.0285
0.4	0.0606
1	1.67

From Fig. 4.6 and Table 4.7 it is inferred that the system performance degrades using 64QAM. The maximum value of the throughput using 64QAM is 1.67 Mbps at 5 MHz bandwidth. It is shown that the throughput increases with the SNR. The maximum

throughput in 5 MHz of system bandwidth and single antenna port is 1.67 Mbps and minimum is 0 Mbps. The results of Fig. 4.6 are summarized in Table 4.7. The throughput performance of QPSK and 16QAM is much better than the 64QAM.

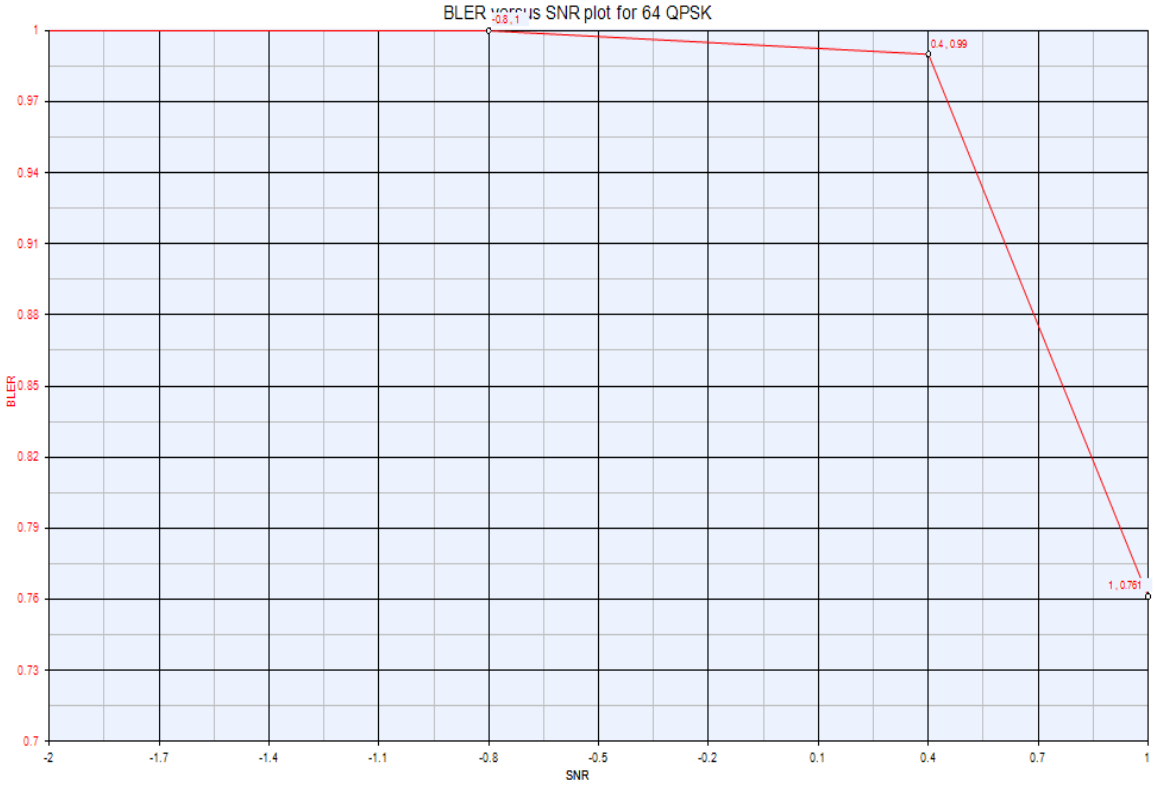

Figure 4.7: Block Error Rate (BLER) v/s SNR plot for 64 QAM.

Table 4.8: BLER and SNR simulation results for 64QAM.

SNR	**Block Error Rate (BLER)**
-2	1
-1.4	1
-0.8	1
-0.2	0.995
0.4	0.99
1	0.761

From Fig. 4.7 and Table 4.8 it is inferred that the system performance degrades using 64QAM. Block Error Rate (BLER) is also an important parameter to measure the performance of communication system, hence in this section the BLER values versus

SNR analysis for 16QAM modulation scheme is demonstrated. Fig. 4.7 shows the simulated graph for BLER versus SNR, for the better performance of the communication system BLER should be mitigated. It is clear from the simulated results that the QPSK and 16QAM performance is much better than the 64QAM. In case of the QPSK and 16QAM the value of the BLER becomes zero and 0.517 respectively at SNR equals to 1, while for the 64QAM it is 0.761.

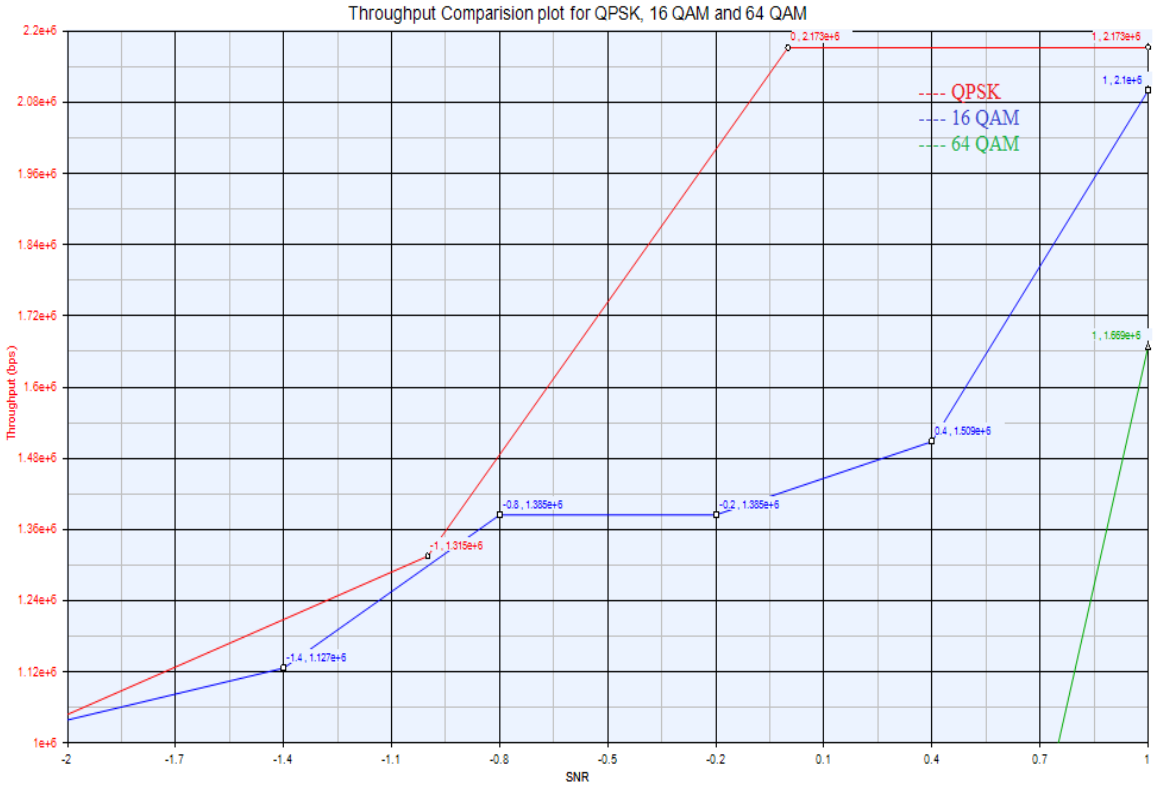

Figure 4.8: Comparison of throughput v/s SNR for QPSK, 16QAM and 64QAM.

Table 4.9: Comparison performance of Throughput for QPSK, 16QAM and 64QAM.

SNR	Throughput (Mbps)		
	QPSK	16QAM	64QAM
-2	1.049	1.039	0
-1.4	1.06	1.127	0
-0.8	1.837	1.385	0
-0.2	2.173	1.385	0.0285
0.4	2.173	1.509	0.0606
1	2.173	2.1	1.67

In Fig. 4.8 and Table 4.9 the performance comparison of channel coding model is done for throughput using different modulation techniques. At a SNR of 1 the throughput of QPSK modulation technique is 2.173 Mbps, for 16QAM at same SNR the required throughput is 2.1 Mbps and for 64QAM at same SNR the throughput is 1.67 Mbps. Hence in order to get same throughput performance, QPSK requires the least SNR.

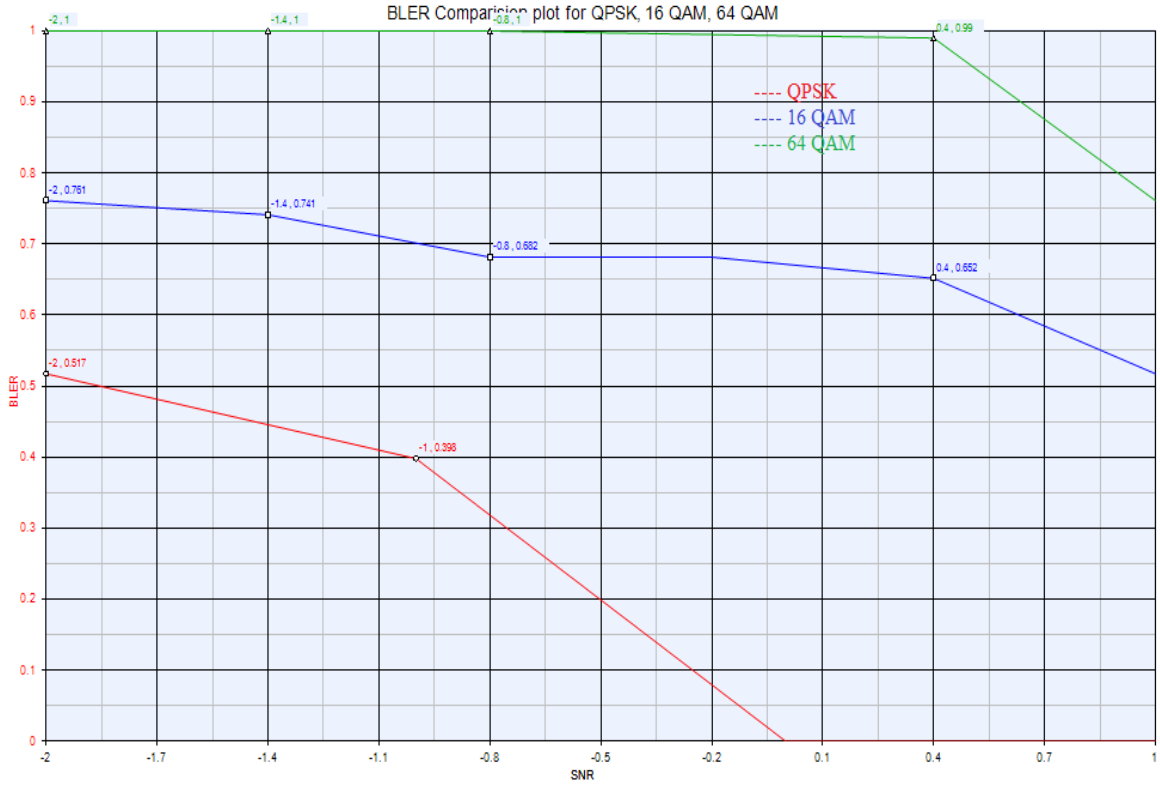

Figure 4.9: Comparison of BLER v/s SNR for QPSK, 16QAM and 64QAM.

Table 4.10: Comparison performance of BLER for QPSK, 16 QAM and 64 QAM.

SNR	Block Error Rate (BLER)		
	QPSK	16 QAM	64 QAM
-2	0.517	0.761	1
-1.4	0.512	0.741	1
-0.8	0.154	0.682	1
-0.2	0	0.682	0.995
0.4	0	0.652	0.99
1	0	0.517	0.761

In Fig. 4.9 and Table 4.10 the performance comparison of system is done for BLER using different modulation techniques. At a SNR of 1 the BLER of QPSK modulation technique is 0, for 16QAM at same SNR the BLER is 0.517 and for 64QAM at same SNR the required BLER is 0.761. Hence in order to get same BLER performance, QPSK requires the least SNR.

4.2 Analysis

The model in chapter 3 for 3GPP channel encoding/decoding works properly for different modulation schemes and by using this model we have analysed the performance of LTE channel encoder and the results are verified with LTE standards. Fig. 4.1 to 4.9 shows FDD downlink throughput in Mbps and BLER for single antenna port and 5 MHz of system bandwidth in QPSK, 16QAM and 64QAM modulation techniques. In these simulations, one OFDM symbol is assigned to PDCCH. The maximum throughput in 5 MHz of system bandwidth, QPSK modulation scheme and one antenna port is 2.173 Mbps; in 5 MHz bandwidth, for 16QAM data modulation maximum throughput is 2.1 Mbps, for 64QAM data modulation and 5 MHz system bandwidth 1.67 Mbps of throughput is possible.

Therefore based on the resource elements we can calculate the maximum throughput of different scenarios by applying the modulation scheme and code rate. These scenarios in FDD downlink can include different channel bandwidths (1.4, 3, 5, 10, 15, 20 MHz), antenna ports (1, 2, or 4). So applying the modulation schemes of 64QAM, 16QAM and QPSK the throughput can be achieved 1.67 Mbps, 2.1 Mbps and 2.173 Mbps respectively.

Besides the throughput calculation, we have calculated the Block Error Rate (BLER) which is an important parameter to measure the performance of the communication system. At a SNR of 1 the BLER of QPSK modulation technique is 0, for 16QAM at same SNR the BLER is 0.517 and for 64QAM at same SNR the required BLER is 0.761. Hence in order to get same BLER performance, QPSK requires the least SNR. The simulation results show that BLER performance of QPSK is better than 16QAM and 64QAM for LTE channel encoding.

CHAPTER

5

CONCLUSION AND FUTURE SCOPE OF THE WORK

5.1 Conclusion

In this dissertation work, an effective study, analysis and performance evaluation of the 3GPP LTE downlink channel coding and decoding using SystemVue software has been carried out. The simulation results i.e. throughput versus SNR and BLER versus SNR was verified by 3GPP LTE standards. In this work an overview of the Long Term Evolution of the UMTS is also presented. LTE intends to support high peak data rates (100 Mb/s in the downlink and 50 Mb/s in the uplink), to improve the system capacity and coverage. It also efficiently supports packet data transmission, etc. OFDM has been adopted as the downlink transmission scheme of LTE. LTE is the future of Mobile broadband. It is expected that in 2014, 80% of broadband users will be mobile broadband subscribers and they will be served by HSPA and LTE networks.

In this work, we have evaluated the performance of LTE downlink channel coding. As channel coding plays a vital role in communication system for error detecting and correcting. During the literature survey, it was found that reference [15] proposed a channel coding model to efficient evaluation of the performance. This model does not give any idea of channel decoding and Hybrid Automatic Repeat Request (HARQ). HARQ model requests to transmitter for retransmitting the corrupted message. In reference [16] both channel coding and decoding model have proposed but no idea of HARQ is given. In this dissertation work, we have proposed an efficient model for performance evaluation of LTE downlink which includes all the three channel coding, channel decoding and HARQ models on a single platform. The performance is evaluated with respect to two definitive metrics namely throughput and BLER for different modulation schemes.

In this work, the throughput and BLER calculation includes both FDD and TDD for uplink and downlink. Moreover, the throughput and BLER analysis can be done for scalable bandwidth (1.4, 3, 5, 10, 15, 20MHz) of LTE and different modulation schemes like QPSK, 16QAM, and 64QAM.

5.2 Future Work

More research still can be done in the LTE downlink channel coding and decoding model because it is a very interesting field. Future work can be done in the order to optimize the throughput in the proposed new channel coding model.

Depending on the goal of the channel coding model we want to design, we may choose to improve the throughput, the fairness or both of them.

The hardware implementation of bandwidth efficient channel coding for LTE is still wide open for research. So naturally, it is a topic of further studies. The hardware implementation can be done using VHDL (or Verilog) for Field Programmable Gate Arrays (FPGA) or by Application Specific Integrated Circuits (ASICs).

It would be worthwhile to evaluate the performance of the LTE downlink with the incorporation of adaptive MIMO switching capabilities. This study was performed for single user scenario.

REFERENCES

[1] M. Rumney, M. J. Pahls, M. Leung, and P. Lorch, "LTE and the evolution to 4G wireless: Design and measurement challenges," U.S.A: Agilent Technologies Publication, 2010.

[2] Agilent Technologies, 3GPP LTE: System overview, product development and test challenges, September 2009.

[3] P. Lescuyer, T. Lucidarme, "Evolved Packet System: The LTE and SAE Evolution of 3G UMTS," John Wiley & Sons Ltd, pp. 159, 2008.

[4] Online Available: http://www.3gpp.org/article/gprs-edge/.

[5] Online Available: http://en.wikipedia.org/wiki/Evolved_HSPA.

[6] J. Zyren, "Overview of the 3GPP Long Term Evolution Physical Layer," White Paper, 2007.

[7] Online Available: http://wiki.hsc.com/LTE_PHY LTEphysicallayerlayer.

[8] Ericsson, LTE-an introduction, White Paper, June 2009.

[9] 3GPP TR 36.212 v9.3.0., Technical Specification Group RAN; Requirements for E-UTRA; Multiplexing and Channel Coding, Release 9.

[10] H Holma, A. Toskala, "LTE for UMTS-OFDMA and SC-FDMA Based Radio Access," John Wiley & Sons Ltd, pp. 71, 2009.

[11] A. Larmo, M. Lindstrom, M. Meyer, G. Pelletier, J. Torsner and H. Wiemann, "The LTE link-layer Design," *IEEE Communications Magazine*, vol.47, no.4, pp. 52-59, April 2009.

[12] D Astely, E. Dahlman, A. Furuskar, Y. Jading, M. Lindstrom, and S. Parkvall, "LTE: the evolution of mobile broadband", *IEEE communication magazine*, April 2009.

[13] Freescale Semiconductor, "Long Term Evolution Protocol Overview," white paper, October 2008.

[14] J. Zyren, W. McCoy, "Overview of the 3GPP Long Term Evolution Physical Layer," white paper by Freescale Semiconductor, June 2007.

[15] T. A. Courtade and R. D. Wesel, "Optimal allocation of redundancy between packet-level erasure coding and physical-layer channel coding in fading channels," *IEEE Trans. Commun.*, vol. 59, no. 8, pp. 2101-2109, Aug. 2011.

[16] S. Zhang and S. C. Liew, “Channel coding and decoding in a relay system operated with physical-layer network coding,” *IEEE Journal on Selected Areas in Commun.*, vol. 27, no. 5, pp. 788-796, Jun. 2009.

[17] E. Rosnes, “On the minimum distance of turbo codes with quadratic permutation polynomial interleavers,” *IEEE Trans. Inf. Theory*, vol. 58, no. 7, pp. 4781-4795, Jul. 2012.

[18] L. Liu, Y. Wang, et al., “Design and implementation of channel coding for underwater acoustic system,” *IEEE Trans. Inf. Theory*, vol. 48, no. 9, pp. 497-500, Sep. 2009.

[19] Y. Cemal and Y. Steinberg, “Coding problems for channels with partial state information at the transmitter,” *IEEE Trans. Inf. Theory*, vol. 53, no. 12, pp. 4521-4536, Dec. 2007.

[20] D. M. Sacristan, et al., “MAC layer performance of different channel estimation techniques in UTRAN LTE downlink,” *IEEE Trans. Commun.*, vol. 53, no. 9, pp. 2256-2261, Sep. 2009.

[21] F. Weng, C. Yin, T. Luo, “Channel estimation for the downlink of 3GPP-LTE systems,” *IEEE Trans. Commun.*, vol. 47, no. 7, pp. 1042-1046, Oct. 2010.

[22] M. Fresia and G. Caire, “A linear encoding approach to index assignment inlossy source-channel coding,” *IEEE Trans. Inf. Theory*, vol. 56, no. 3, pp. 1322-1344, Mar. 2010.

[23] D. Gunduz, et al., “Source and channel coding for correlated sources over multiuser channels,” *IEEE Trans. Inf. Theory*, vol. 55, no. 9, pp. 3927-3944, Sep. 2009.

[24] J. J. Sanchez, D. M. Jimenez, G. Gomez, J. T. Enbrambasaguas, “Physical Layer Performance of Long Term Evolution Cellular Technology,” 16th IST Mobile and Wireless Communications Summit, 2007.

[25] E. Virtej, M. Kuusela, E. Tuomaala, “System Performance of Single-User MIMO in LTE Downlink,” *IEEE 19th International Symposium,* Sept. 2008.

[26] D. M. Sacristan, J. Cabrejas, D. Calabuig, J. F. Monserrat, “MAC Layer Performance of Different Channel Estimation Techniques in UTRAN LTE Downlink,” *IEEE 69th Vehicular Technology Conference (VTC),* Jun. 2009.

[27] D.M. Sacristan, J. F. Monserrat, J. Cabrejas, D. Calabuig, S. Garrigas, N. Cardona, “On the Way towards Fourth-Generation Mobile: 3GPP LTE and LTE-Advanced,” *EURASIP Journal on Wireless Communications and Networking*, July 2009.

[28] 3GPP R1-072261, “LTE Performance Evaluation-Uplink Summary,” May 2007.

[29] 3GPP R1-072578, “Summary of Downlink Performance Evaluation,” May 2007.

[30] A. Furuskar, T. Jonsson, M. Lundevall, “The LTE Radio Interface key Characteristics and Performance,” Personal, IEEE Indoor and Mobile Radio Communications, September 2008.

[31] C. Ball, T. Hindelang, I. Kambourov, S. Eder, “Spectral Efficiency Assessment and Radio Performance Comparison between LTE and WiMAX ,” *IEEE Communication Letter*, vol. 5, no. 6, pp. 239-241, Sep. 2008.

[32] Q. Li, G. Li, W. Lee, M. Lee, D. Mazzarese, B. Clerckx, and S. Z. Li, “MIMO Techniques in WiMAX and LTE: A Feature Overview,” *IEEE communication Magazine*, vol. 23, no. 13, pp. 423-28, May 2010.

[33] Y. Yang, H. Hu, J. Xu, G. Mao, “Relay Technologies for WiMAX and LTE-Advanced Mobile Systems,” *IEEE Communications Magazine*, vol. 47, no. 10, pp. 100-105, Oct. 2009.

[34] A. Ghosh, R. Ratasuk, B. Mondal, N. Mangalvedhe, T. Thomas, “LTE-Advanced: next-generation wireless broadband technology,” *IEEE Communication Letter*, vol. 7, no. 9, pp. 327-332, Jun. 2010.

[35] M. Iwamura, K. Etemad, M.H. Fong, R. Nory, and R. Love, “Carrier Aggregation Framework in 3GPP LTE-Advanced,” *IEEE communication Magazine*, vol. 67, no. 13, pp. 437-442, Aug. 2010.

[36] K. Kusume, G. Dietl, T. Abe, H. Taoka, and S. Nagata, “System Level Performance of Downlink MUMIMO Transmission for 3GPP LTE-Advanced,” *IEEE 71st Vehicular Technology Conference (VTC)*, Jun. 2010.